공학박사 학위논문

Promoted Differentiation of Mesenchymal Stem Cells using a Stretchable Piezoelectric Substrate for Regeneration of Myocardium and Skeletal Muscle

압전탄성 배양표면에 의해 분화가 촉진된 중간엽 줄기세포의 심근 및 골격근 재생효과

2017년 8월

서울대학교 공과대학

화학생물공학부

윤 정 기

Abstract

Promoted Differentiation of Mesenchymal Stem Cells using a Stretchable Piezoelectric Substrate for Regeneration of Myocardium and Skeletal Muscle

Jeong-Kee Yoon

School of Chemical and Biological Engineering

The Graduate School

Seoul National University

In native muscle microenvironment, electrical and mechanical stimuli exist in the form of action potential and muscle contraction. Here we developed a cell culture system that can mimic the *in vivo* microenvironment and provide these stimuli to cultured cells and investigated whether the stimulation can promote myogenic differentiation of human mesenchymal stem cells (hMSCs). *Ex vivo* induction of myogenic differentiation of MSCs prior to implantation would potentiate therapeutic efficacy of stem cell therapies for muscle diseases, since MSCs rarely undergo myogenic differentiation following implantation. In muscle microenvironments, electric pulse and cyclic mechanical strain are sequentially produced. However, no study has applied the pulsatile mechanoelectric cues

(PMEC) to stimulate myogenic differentiation of MSCs *ex vivo*. Stretchable and piezoelectric substrate (SPS) was fabricated by polydimethylsiloxane spin-coating on aligned ZnO nanorods. PMEC were provided to hMSCs cultured on SPS by subjecting SPS to cyclic stretching and bending, resulting in significantly promoted myogenic differentiation of hMSCs as well as intracellular signaling related to the differentiation. There are three types of muscle in human body: cardiac muscle, skeletal muscle, and smooth muscle. In the present study, we have focused on hMSCs differentiation into cardiac muscle cells and skeletal muscle cells in part 3 and 4, respectively. In part 3, bone marrow-derived hMSCs were induced to differentiate into cardiomyocytes to confirm the efficiency of PMEC for myogenic differentiation. Furthermore, in part 4, human umbilical cord blood MSCs were induced to differentiate into skeletal myocyte on pNIPAAm-engrafted thermosensitive SPS (TSPS). Following differentiation *ex vivo*, the cells were detached from TSPS in the form of cell-sheet fragments by changing the temperature to 4℃. The injection of cell-sheet fragments of differentiated cells into injured skeletal muscle in mice showed improved cell retention and muscle regeneration compared to injection of either undifferentiated cells or differentiated/dissociated cells. Our system may provide a tool for study of electrical and mechanical regulation of stem cells and be utilized to potentiate stem cell therapies.

Keywords : human mesenchymal stem cells, myogenic differentiation, muscle disorders, pulsatile mechanoelectric cues, cell sheet

Student Number **: 2012-23270**

Table of contents

List of figures

Abbreviations

5-azaC	5-azacytidine
ANOVA	analysis of variance
ATF6	activating transcription factor
BCL-2	B-cell CLL/lymphoma 2
bFGF	basic fibroblast growth factor
BMP	bone morphogenetic protein
BMSC	bone marrow-derived mesenchymal stem cell
CACNA1C	voltage-dependent, L type, alpha 1C subunit
cDNA	complementary DNA
CM	cell membrane
CTX	cardiotoxin
Cx43	connexin43
DAPI	4,6-diamidino-2-phenylindole
ECM	extracellular matrix
EDL	electrical double layer
EP	electric pulse
ER	endoplasmic reticulum

ERK1/2	extracellular signal-regulated kinases 1/2
FAK	focal adhesion kinase
FITC	fluorescein isothiocyanate
GATA4	GATA binding protein 4
grp78	glucose-regulated protein 78 kDa
H&E	hematoxylin and eosin
HCN2	cyclic nucleotide-gated potassium channel 2
HMTA	hexamethylenetetramine
HNA	human nuclear antigen
hsp27	heat shock protein 27
hUCBMSC	human umbilical cord blood-derived mesenchymal stem cell
IACUC	Institutional Animal Care and Use Committee
IGF	insulin-like growth factor
MEF-2	myocyte enhancer factor 2
MRFs	myogenic regulatory factors
MS	mechanical strain
MSC	mesenchymal stem cell
mTOR	mammalian target of rapamycin
Myh1	myosin heavy chain 1

Myh2	myosin heavy chain 2
NKX 2.5	NK2 homeobox 5
nNOS	neuronal nitric oxide synthase 1
PBS	phosphate buffer saline
PDMS	polydimethylsiloxane
pERK1/2	phosphorylated extracellular signal-regulated kinases 1/2
pFAK	phosphorylated focal adhesion kinase
PMEC	pulsatile mechanoelectric cues
pmTOR	phosphorylated mammalian target of rapamycin
pNIPAAm	poly(N-isopropylacrylamide)
PP	piezoelectric pulse
pp38	phosphorylated p38
pSMAD	phosphorylated SMAD
qPCR	quantitative polymerase chain reaction
RhoA	Ras homolog family member A
RNA	ribonucleic acid
RT-PCR	reverse transcription polymerase chain reaction
SDS	sodium dodecyl sulfate
SEM	scanning electron microscope

SPS	stretchable piezoelectric substrate
SWCNT	single-walled carbon nanotubes
TA	tibialis anterior
TBPO	tert-butyl peroxide
TCP	tissue culture plate
TEM	transmission electron microscope
TGF-β	transforming growth factor-β
TRITC	rhodamine
TSPS	thermosensitive, stretchable, and piezoelectric substrate
VEGF	vascular endothelial growth factor
V_{mem}	cell membrane potential
XPS	X-ray photoelectron spectroscopy
ZnO NRs	zinc oxide nanorods
β-MHC	beta myosin heavy chain

Chapter 1.

Research backgrounds and objective

1.1. Cardiovascular diseases and stem cell therapy

When cardiovascular diseases, such as myocardial infarction occur, cardiomyocytes undergo apoptosis and necrosis due to lack of nutrients or oxygen.[1] The major problem of these cardiovascular diseases is that only a few cardiomyocytes regenerate in infarcted area and are progressively replaced by fibroblasts to form scar tissues.[2] The host cells are not able to fully reconstitute the fibrotic tissue and overcome cardiac malfunction due to this massive loss of functional cardiomyocytes, and these problems leads to chronic heart diseases or death.

To treat such cardiovascular diseases, heart transplantation has been a therapy for several decades, however, it has severe limitation by the shortage of donors and the host immune rejection. To overcome such problems, cell therapy, especially stem cell therapy, has been widely studied in this century. The role of the transplanted stem cell in infarcted area is still unknown, but blood vessel formation, scar tissue reduction, or secretion of beneficial growth factors or cytokines are suggested.[3-4]

Also, some of the studies tried to differentiate the stem cell into functional cardiomyocytes *ex vivo* before transplantation, using embryonic stem cells. Although embryonic stem cells have shown a good functional performance, the embryonic stem cells have a severe limitation for being transplanted *in vivo*, such as teratoma formation.[5] To overcome such problems, mesenchymal stem cells (MSCs) is being studied as an alternative. Unlike other adult stem cells, MSCs can evade from innate immune system and have immune-modulating properties, thus making them possible for allogeneic stem cell therapy.[6] However, when the MSCs

were transplanted into infracted area, these cells hardly differentiate into functional cardiomyocytes *in vivo*, indicating that transplantation of undifferentiated MSCs may not be the best approach for cardiac regeneration.[3, 7] Thus the differentiation of MSCs into functional cardiomyocytes has been widely studied, while the capability of MSCs differentiating into functional cardiomyocytes is still controversial.

1.2. Skeletal muscle disorders and stem cell therapy

Functional loss of skeletal muscle tissue due to trauma, aging, genetic problem, or degenerative muscle disorders, such as sarcopenia and muscular dystrophy, have significant clinical problems in human society. Several clinical trials have been developed, however, they were not much efficient due to morbidity of target tissues.

Spontaneous regeneration of adult skeletal muscle is regulated by the differentiation of myogenic precursor cells, termed satellite cells, which are quiescent in normal state.[8-9] Under abnormal conditions, the satellite cells proliferate as myogenic precursor cells, termed myoblasts, and ultimately undergo terminal differentiation and fuse to each other to form new myotubes or incorporate into pre-existing muscle fibers.

There have been many therapeutic challenges for treatment of such skeletal muscle disorders, especially cell therapy, as many skeletal muscle disorders are caused by severe degeneration compared to satellite cell proliferation and differentiation.[10] First, myoblasts have been suggested to be transplanted into patients, resulting only low therapeutic efficiency by poor cell survival, immune rejection, poor migration *in vivo*, and slow proliferation in *vitro*.[11-12] To overcome such problems, adult stem cells such as MSCs have been a candidate source for skeletal muscle regeneration. Although stem cells transplantation have shown better regeneration efficiency than myoblasts, the frequency of incorporation into skeletal muscle was still not high enough.[13]

1.3. Cardiomyogenic and skeletal myogenic differentiation of MSCs

As MSCs hardly function or incorporate into cardiac muscle tissue or skeletal muscle tissue transplanted *in vivo*, MSCs have to be primed or be differentiated into cardiomyocytes or skeletal myocytes.

To differentiate MSCs into cardiomyocytes, treatments with 5-azacytidine (5-azaC),[14-15] growth factors such as transforming growth factor-β (TGF-β),[16] basic fibroblast growth factor (bFGF), insulin-like growth factor-1 (IGF-1), and bone morphogenetic protein-2 (BMP-2),[17] conditioned medium from cardiomyocyte culture,[18] and by co-culture with cardiomyocytes.[19] However, chemical factors, such as 5-azaC, are able to promote cardiomyogenic differentiation of MSCs (Fig. 1.1), the efficiency is known to be relatively low.

For skeletal myogenic differentiation of MSCs, some methods such as development of myogenic medium,[20-21] culturing cells in three-dimensional scaffold,[22] and expose to laser irradiation[23] have been developed, by their efficiency of differentiation (Fig. 1.2) was also relatively low.

Recently, several studies have demonstrated that mimicking native muscle microenvironment, such as electrical[24-25] and mechanical stimulation[26-27] can promote myogenic differentiation of the stem cells. However, there was no study which simultaneously subject electrical and mechanical stimulation to MSCs for myogenic differentiation, neither for cardiomyogenic lineage nor skeletal myogenic lineage, and the mechanism of both stimulations were not clarified.

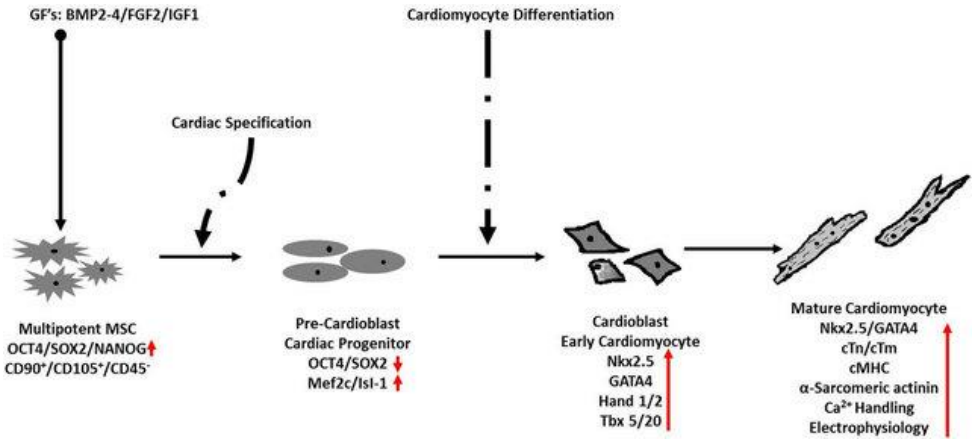

Figure 1.1. Illustration of expected stages of cardiomyogenesis in MSCs.[28]

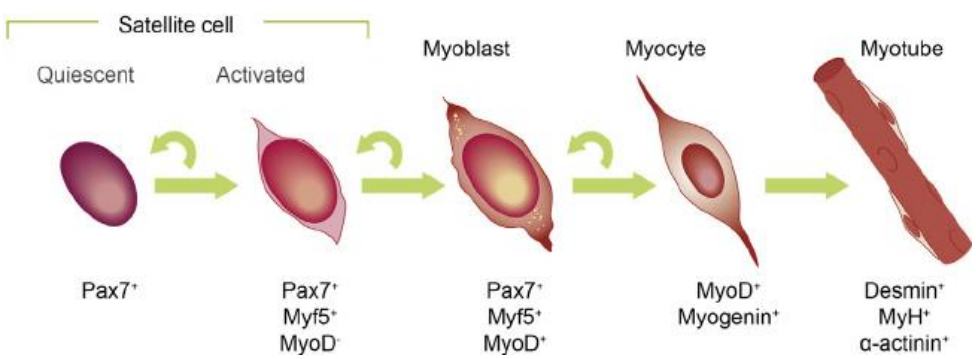

Figure 1.2. Differentiation progression during adult myogenesis: from satellite cells to differentiated myotubes.[29]

1.4. Piezoelectricity

In the present study, we developed a stretchable piezoelectric substrate (SPS) for myogenic differentiation of hMSCs. SPS consists of aligned bi-axially grown ZnO NRs which have piezoelectricity, and polydimethylsiloxane (PDMS) which has elasticity.

Piezoelectricity is the electric charge that accumulates in certain solid materials, in response to applied mechanical stress. The piezoelectric effects of piezoelectric materials are closely related with the electric dipole moments. When a mechanical stress is applied, the polarization of the dipole moment changes to generate piezoelectric effect. In our study, we used bi-axially grown zinc oxide nanorods (ZnO NRs) for piezoelectric property of SPS. ZnO has a hexagonal wurzite structure, which have a permanent dipole moment in the positive direction along the c-axis (Fig. 1.3). The ZnO NRs can be bi-axially or uni-axially grown, however, when the uni-axially grown ZnO NRs were bent, the net potential of the ZnO NRs becomes zero as shown in figure 1.4. On the other hand, when the bi-axially grown ZnO NRs were convexly bent, positive charge is generated in a convex direction as shown in figure 1.5.

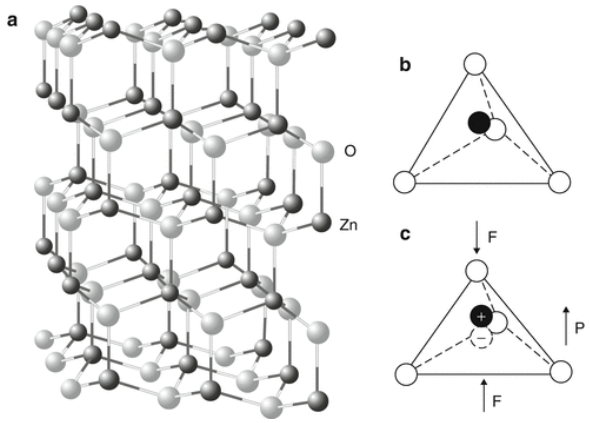

Figure. 1.3. Wurzite structure of ZnO and induced dipole moment through mechanical stress

Figure 1.4. When uni-axially grown ZnO NRs is convexly bent, the net potential is zero.

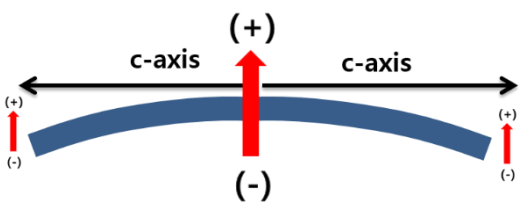

Figure 1.5. When bi-axially grown ZnO NRs is convexly bent, positive charge is generated in a convex direction.

1.5. Thermosensitivity and cell sheet formation

As previously mentioned, cell therapy has been widely used for muscle disorders, such as myocardial infarction or skeletal muscle degeneration. However, when the cells are transplanted *in vivo*, the poor survival of the transplanted cells has been a severe problem, such as anoikis. [30-32] Anoikis means programmed cell death of anchorage-dependent cells, occurred when they are detached from the surrounding extracellular matrix (ECM). To prevent anoikis, various methods have been devised, such as three dimensional culture as cell spheroid, [31] or cell sheet formation.[32] In part 4, the skeletal myogenic differentiated cells were transplanted as a form of cell sheet fragments to prevent anoikis.

We have grafted poly(N-isopropylacrylamide) (pNIPAAm) which has thermosensitivity on the surface of SPS to fabricate TSPS. pNIPAAm is a thermosensitive polymer, which undergoes a reversible phase transition from a swollen hydrophilic state to a shrunken hydrophobic state, when it is heated above 32℃. pNIPAAm has been widely used in tissue engineering, as the temperature of the reversible phase transition is near that of the human body.

In the present study, the cells cultured and differentiated on TSPS in chapter 4, were detached as a cell sheet and sliced into smaller fragments to be injected with syringe, to increase engraftment efficiency and prevent anoikis.

1.6. Research objective of thesis

The research objective in this thesis is the enhancement of the myogenic differentiation efficiency of hMSCs, for stem cell therapy to treat muscle disorders, such as myocardial infarction or skeletal muscle degeneration.

Firstly, the chapter 3 reports the enhanced cardiomyogenic differentiation of bone marrow-derived hMSCs using SPS. In cardiac microenvironments, electric pulse and cyclic mechanical strain are sequentially produced. However, no study has applied the pulsatile mechanoelectric cues (PMEC) to stimulate cardiomyogenic differentiation of MSCs *ex vivo*. We developed the SPS that can provide PMEC to hMSCs for cardiomyogenic differentiation *ex vivo*. We showed that hMSCs subjected to PMEC by SPS underwent promoted cardiac phenotype development; cell alignment and the expression of cardiac markers (i.e., cardiac transcription factors, structural proteins, ion channel proteins, and gap junction proteins). The enhanced cardiac phenotype development was mediated by the up-regulation of cardiomyogenic differentiation-related autocrine factor expression and focal adhesion kinase and extracellular signal-regulated kinases signaling pathways. *Ex vivo* induction of cardiomyogenic differentiation of hMSCs using SPS prior to implantation would potentiate therapeutic efficacy of stem cell therapies for ischemic heart diseases, since MSCs rarely undergo cardiomyogenic differentiation following implantation.[33] However, we did not observed the *in vivo* therapeutic efficacy of cardiomyogenic differentiated hMSCs.

Secondly. The chapter 4 reports the skeletal myogenic differentiation of human umbilical cord blood-derived hMSCs (hUCBMSCs) using TSPS. In native muscle microenvironment, electrical and mechanical stimuli exist in the form of action

potential and muscle contraction. We developed a cell culture system that can mimic the *in vivo* microenvironment and provide these stimuli to cultured cells and investigated whether the stimulation can promote skeletal myogenic differentiation of hUCBMSCs. TSPS was fabricated by subsequent grafting pNIPAAm on the polydimethylsiloxane surface of SPS. PMEC were provided to hUCBMSCs cultured on TSPS by subjecting TSPS to cyclic stretching and bending, resulting in significantly promoted skeletal myogenic differentiation of hUCBMSCs as well as intracellular signaling related to the differentiation. Following differentiation *ex vivo*, the cells were detached from TSPS in the form of cell-sheet fragments by changing the temperature to 4℃. The injection of cell-sheet fragments of differentiated cells into injured skeletal muscle in mice showed improved cell retention and muscle regeneration compared to injection of either undifferentiated cells or differentiated/dissociated cells. This system may provide a tool for study of electrical and mechanical regulation of stem cells and be utilized to potentiate stem cell therapies.

Chapter 2.

Experimental methods

2.1. Fabrication and characterization of SPS, TSPS

2.1.1. Chemicals

Zinc nitrate hexahydrate ($Zn(NO_3)_2 \cdot 6H_2O$, $\geq$ 99.0 %), hexamethylenetetramine (HMTA) ($C_6H_{12}N_4$, $\geq$ 99.0 %) and anhydrous hexane were purchased from Sigma Aldrich (St. Louis, MO, USA). Zinc nitrate hexahydrate and HMTA were dissolved in deionized water by stirring for 30 min prior to use. Sylgard 184 PDMS prepolymer and curing agents were purchased from Dow Corning Chemicals (Midland, MI, USA).

2.1.2. Synthesis of bi-axially grown ZnO NRs

A wet chemical process was used to prepare bi-axially grown ZnO NRs.[34] Two precursor solutions were prepared by separately dissolving 0.42 g of zinc nitrate hexahydrate in 100 mL of deionized water and 0.24 g of HMTA in 100 mL of deionized water at room temperature. The zinc precursor solution was continuously injected into the HMTA solution with vigorous stirring at 85 ℃ via a syringe pump at an injection rate of 2 mL/hr for 25 min, and the process was completed after aging for 5 min. After synthesis, ZnO NRs were washed three times with deionized water and dried at 80 ℃. Finally, the ZnO NR powder was thermally annealed at 400 ℃ for 2 hr in vacuum to increase crystallinity.

2.1.3. Fabrication of SPS

Before the PDMS was used (PDMS:PDMS curing agent weight ratio = 10:1), PDMS and hexane were mixed to control the film thickness of PDMS (PDMS:hexane weight ratio = 1:1). The PDMS and hexane mixtures were spin-coated at 3,000 rpm for 30 sec. A monolayer of ZnO NRs was formed using a unidirectional rubbing process with a PDMS block on the PDMS substrate. This procedure was repeated five or three times to make a one-direction array and close-packed SPS with five layers of ZnO NRs that generated 3 V or 120 mV. 3 mm of PDMS was prepared for before stacking 5 layers fabricating of SPS, and each layer, consisting of ZnO NRs and PDMS, was 5 μm-thick. The thickness and electrical properties were evaluated after SPS formation.

2.1.4. pNIPAAm grafting

GMA monomer (97%) and the tert-butyl peroxide (TBPO) initiator (98%) were purchased from Sigma-Aldrich and used without further purification. Polymerized GMA films were deposited onto the stretchable piezoelectric substrate in an iCVD reactor (Daeki Hi-Tech Co., Korea). GMA monomer was heated to 35 ℃ and the vaporized GMA was fed into the reactor at a flow rate of 1.9 sccm for coating the pGMA film on the stretchable piezoelectric substrate. The vaporized TBPO initiator was fed into the reactor *via* metering valves at a flow rate of 0.8 sccm at room-temperature. In order to keep the stretchable piezoelectric substrate at 25 ℃ during the pGMA coating process, the substrates were placed on a stage cooled by a recirculating chiller. The filament temperature was maintained at 180 ℃. The growth rate of film deposition was monitored *in situ* using a He-Ne laser (JDS Uniphase, Milpitas, USA). Amine-terminated pNIPAAm (Mn = 2500, Sigma-Aldrich Co.) was dissolved in deionized (DI) water at a concentration of 1 g/30 mL. The pNIPAAm solution was reacted with the pGMA deposited the stretchable piezoelectric substrate through epoxy-amine addition reaction in a shaker at 50 ℃ for 12 h at 55 rpm. Next, it was washed several times with DI water. Prior to cell seeding, substrates were sterilized with 70% (v/v) ethanol and UV treated for 1 h on a clean bench.

2.1.5. Piezoelectric properties of SPS and TSPS

The morphology of the ZnO NRs was characterized with a JEOL JSM-7000F field emission SEM (FESEM, Jeol Ltd, Akishima, Tokyo, Japan; 15 kV). To evaluate the electrical properties of the SPS, silver electrodes (200 nm) were deposited on the top and bottom sides of the SPS by thermal evaporation. The silver electrode was not used for cell culture. After placing the device on the 3-mm thick PDMS substrate, voltage and current signals were measured. The SPS was then bent with a 20 mm bending radius, and the current density and voltage generated were measured using a picoammeter (Keithley 6485, Keithley Instruments, Cleveland, OH, USA) and electrometer/high resistance meter (Keithley 6517, Keithley Instruments), respectively. It is not possible to experimentally acquire values of voltage and current at the same time, since the measured voltage is an open circuit voltage and the measured current is a short circuit current. Five samples were used for evaluation of electrical properties in this study. The deviation of voltage and current between samples was less than 10 %. Permanent deformations of SPS and PDMS were determined by comparing the length after cyclic bending or cyclic bending/stretching (n = 3) to the original length. ZnO NR alignment in the SPS was evaluated on day 0 and after 10 days of cyclic bending and stretching using 5 images photographed at random sites on the substrate using an optical microscope (BX41, Olympus, Tokyo, Japan). The alignment was analyzed using Image J software (National Institute of Health, Bethesda, MD, USA).

2.1.6. Thermosensitivity of TSPS

The chemical composition and atomic ratio of PDMS, pGMA-PDMS and pNIPAAm-pGMA-PDMS surface was analyzed by X-ray photoelectron spectroscopy (XPS, K-alpha, Thermo VG Scientific Inc, UK). The vacuum base pressure was maintained at 2.0×10^{-9} mb. The spectrum was recorded with a monochromatic Al Kα radiation X-ray source having 12kV and 1486.6eV KE with the range of 100 – 1100 eV. The atomic ratio of each surface was determined by Avantage program (Thermo Scientific).

To evaluate the thermosensitivity of TSPS, the TSPS was characterized using contact angle measurements, in two different temperatures, 25℃ and 37℃. Deionized water droplet (2 μL) was delivered on the TSPS surface by a calibrated syringe. To test the detachment of the attached cells, the cells on TSPS were cooled down to 4 ℃ for 10 min, being dipped in cold PBS. The cell detachment was observed using an image analysis system coupled to a light microscope.

2.2. *In vitro* assays

2.2.1. hMSC culture and cardiomyogenic differentiation

hMSCs (Lonza, Walkersville, MD, USA) were plated at 5 x 10^4 cells/cm^2 on tissue culture plate (TCP) and various types of substrates, and cultured. To promote cell attachment to the surfaces of TCP and the substrates, the surfaces were treated with oxygen plasma (60 W, PDC-32G, Harrick Scientific, Ossining, NY, USA) for 1 min. hMSCs were cultured with Dulbecco's Modified Eagle Medium low glucose (Gibco BRL, Gaithersburg, MD, USA) supplemented with 10 % (v/v) fetal bovine serum (Gibco BRL) and 1 % (v/v) penicillin/streptomycin (Gibco BRL) at 37 ℃ in a humidified incubator with 5 % (v/v) CO_2. hMSCs at 5 passages were used for the experiments. hMSCs were pre-treated with 5-azaC (6 μmol/L) for 1 day. Cells were allowed to adhere to the substrates for 1 day, and subjected to cyclic bending at a 20 mm bending radius and 1 Hz frequency, and cyclic stretching at an amplitude of 3 % of the original length of the substrates and 1 Hz frequency for 10 days using a custom-made cell culture apparatus. We used 1 Hz frequency, because this frequency is similar to human heartbeat rate, as we used human-derived cells for cardiomyogenic differentiation. The culture medium was changed every 3 days.

2.2.2. hUCBMSC culture and skeletal myogenic differentiation

hUCBMSCs (Kangstem Biotech, Seoul, Korea) were plated at 5 x 10^4 cells/cm^2 on TSPS and cultured. To promote cell attachment on TSPS, TSPS was treated with oxygen plasma (60 W, PDC-32G, Harrick Scientific, Ossining, NY, USA) for 1 min. hUCBMSCs were cultured with Dulbecco's Modified Eagle Medium low glucose (Gibco BRL, Gaithersburg, MD, USA) supplemented with 10 % (v/v) fetal bovine serum (Gibco BRL) and 1 % (v/v) penicillin/streptomycin (Gibco BRL) at 37 ℃ in a humidified incubator with 5 % (v/v) CO_2. hUCBMSCs at 5 passages were used for the experiments. For skeletal myogenic differentiation, myogenic medium consisting of Dulbecco's Modified Eagle Medium low glucose, 5 % horse serum, 0.1 μM dexamethasone, and 50 μM hydrocortisone was used.[20] To inhibit calcium influx, 10 μM of nifedipine (Sigma) was added to myogenic medium. Cells were allowed to adhere to TSPS for a day and subjected to cyclic bending (36 mm bending radius) and/or cyclic stretching (amplitude of 3 % of the original length of the substrate) at 0.3 Hz frequency for 10 days using a custom-designed cell culture chamber. The external stimulation conditions were adjusted to conditions that did not induce apoptotic effects or cell detachment, but promote myogenic differentiation. Also, we used a shorter time point than previous study,[20] 10 days, to confirm the higher efficiency of our method for myogenic differentiation.

2.2.3. Immunocytochemistry

The cells on the substrates (n = 3) were fixed with 4 % paraformaldehyde for 10 min at room temperature and washed in phosphate buffer saline (PBS, Gibco-BRL). Primary antibodies against caspase-3, connexin43 (Cx43), sarcomeric α-actinin, myogenin (all antibodies from Abcam) were used for staining. The samples were then incubated in PBS containing rhodamine (TRITC) or fluorescein isothiocyanate (FITC)-conjugated secondary antibodies (Jackson-Immunoresearch, West Grove, PA, USA) for 1 hr at room temperature. All samples were mounted with mounting solution containing 4,6-diamidino-2-phenylindole (DAPI, Vector Laboratories, Burlingame, CA, USA) to stain the nuclei, and photographed using a fluorescent microscope (Olympus, Tokyo, Japan).

2.2.4. Reverse transcription polymerase chain reaction (RT-PCR)

RT-PCR was used to compare the relative gene expressions of *CASPASE-3, BCL-2, P53, BMP-4, TGF-β, VEGF,* and *IGF*. Samples (n = 4) were lysed with TRIzol reagent (Invitrogen, Carlsbad, CA, USA). Total ribonucleic acid (RNA) was extracted with chloroform (Sigma) and precipitated with 80 % (v/v) isopropanol (Sigma). After the supernatant was removed, the RNA pellet was washed with 75 % (v/v) ethanol, air-dried, and dissolved in 0.1 % (v/v) diethyl pyrocarbonate-treated water (Sigma). RNA concentration was determined by measuring the absorbance at 260 nm with a NanoDrop 2000 Spectrophotometer (Thermo Scientific, Wilmington, DE). Reverse transcription was performed using 5 μg of pure total RNA and SuperScript™ II reverse transcriptase (Invitrogen), followed by PCR amplification of the synthesized complementary DNA (cDNA). PCR consisted of 35 cycles of denaturing (94 ℃, 30 sec), annealing (58 ℃, 45 sec), and extending (72 ℃, 45 sec), with a final extension at 72 ℃ for 10 min. PCR was followed by electrophoresis on 2 % (w/v) agarose gel and visualized using ethidium bromide staining. PCR products were analyzed using a gel documentation system (Gel Doc 1000, Bio-Rad, Hercules, CA, USA). β-actin served as the internal control. The RT-PCR results were quantified with an Imaging Densitometer (Bio-Rad).

2.2.5. Phalloidin staining

Phalloidin staining was performed to determine F-actin alignment and cell fusion, using an Actin Cytoskeleton and Focal Adhesion Staining Kit (FAK100; Millipore, Billerica, MA) according to the manufacturer's instructions. The images were photographed using a fluorescent microscope (Olympus). The average number of nuclei per cell was quantified by dividing the number of nuclei to the number of cell body ($n > 100$). The fused cell percentage was determined by dividing the number of multinucleated nuclei to the total number of nuclei analyzed ($n > 100$). The angle of the F-actin-stained cell alignment to the direction of the MS was determined using Image J software (National Institute of Health, Bethesda, MD).

2.2.6. Western blot analysis

Apoptotic activity, cardiomyogenic differentiation, skeletal myogenic differentiation, and molecular signaling were evaluated by detecting relevant protein markers using western blot analysis. Cells (n = 4) were washed three times with PBS, lysed by adding sodium dodecyl sulfate (SDS) sample buffer (62.5 mM Tris–HCl (pH 6.8), 2 % SDS, 10 % glycerol, 50 mM dithiothreitol, 0.1 % Bromophenol Blue), and scraped. Proteins in the buffer were electrophoretically separated on 4-10 % SDS polyacrylamide gels and transferred to membranes (Millipore, Bedford, MA, USA). For protein detection, membranes were incubated with primary antibodies against caspase-3, Cx43, NKX2.5, MEF-2, GATA4, sarcomeric α-actinin, β-MHC, p38, pp38, SMAD, pSMAD, FAK, pFAK, ERK1/2, pERK1/2, MyoD, myogenin, troponin I, ATF6, RhoA, nNOS, mTOR, pmTOR, and β-actin (all antibodies from Abcam, Cambridge, MA, USA), overnight at 4 °C. They were then washed and incubated with secondary antibodies conjugated to horseradish peroxidase (Sigma) for 50 min at room temperature. Blots were developed using enhanced chemiluminescence (LumiGLO, KPL Europe, Guildford, UK) as recommended by the manufacturer.

2.2.7. Quantitative polymerase chain reaction (qPCR)

qRT-PCR was used to quantify relative gene expression of ion channel markers, *HCN2* and *CACNA1C*, and skeletal myogenic differentiation markers, MyoD, Myogenin, MEF2, troponin I and myosin heavy chain 1 and 2. Total RNA was extracted from samples (n = 4) using 1 mL Trizol reagent (Invitrogen) and 200 μL of chloroform. The lysed samples were centrifuged at 12,000 rpm for 10 min at 4 ℃. The RNA pellet was washed with 75 % (v/v) ethanol in water and dried. After drying, samples were dissolved in RNase-free water. For qRT-PCR, the iQ™ SYBR Green Supermix kit (Bio-Rad) and the MyiQ™ single color Real-Time PCR Detection System (Bio-Rad), were used. β-actin served as the internal control.

2.2.8. Transmission electron microscope (TEM)

Cells were fixed using Karnovsky's fixative for 4 h at 4 ℃ and rinsed three times with cold 0.05 M cacodylate buffer. The cells were fixed with 1 % osmium tetraoxide for 2 hr at 4 ℃ and washed twice with cold distilled water. The samples were treated with 0.5 % uranyl acetate overnight at 4 ℃, dehydrated using graded concentrations of ethanol (30, 50, 70, 80, 90, 95, and 100%), rinsed with propylene oxide, and finally embedded in Spurr's resin, which were then polymerized at 70 ℃ for 24 hr. Thin sections with thicknesses of 100 nm were obtained using an ultramicrotome (Leica), collected on 200-mesh copper grids, and observed using a TEM (JEM-1010, JEOL Ltd.).

2.2.9. Fragmentation of cell sheet

After hUCBMSCs were stimulated for myogenic differentiation for 10 days, the cell sheets were detached from TSPS by cooling down at 4 ℃. The detached cell sheets were chopped into small cell sheet fragments (diameter = 94.9 ± 30.2 μm) for syringe injection and labeled with DiI. The cell sheet fragments were mounted with mounting solution containing DAPI (Vector Laboratories) to stain the nuclei. The cell sheets were photographed using a fluorescent microscope (Olympus). The size of cell sheet fragments and number of nuclei per cell sheet fragments were quantified using Image J software (National Institute of Health).

2.3. *In vivo* assays

2.3.1. Inducing skeletal muscle injury and cell transplantation.

All animal experiments were performed under a protocol approved by the Institutional Animal Care and Use Committee (IACUC) of Seoul National University (SNU-160720-12). For muscle injury induction, 9 week-old female balb/c athymic nude mice (Orient Bio, Seoul, Korea) (n = 5 mice per group) were anesthetized with xylazine (10 mg/kg) and ketamine (100 mg/kg), and 50 μL of 1 mM cardiotoxin (CTX, Latoxan, Rosans, France) was administered into the right TA muscles of mice. One day after CTX injection, cells ($2x10^5$ cells/mouse) or PBS were intramuscularly injected with 24-gauge syringe.

2.3.2. Histological examinations

Ten and 28 days after cell transplantation, the TA muscles were harvested and embedded in OCT compound. The embedded tissues were cut in 10 μm sections and stained with hematoxylin and eosin (H&E) or underwent to immunohistochemistry against laminin, troponin I, desmin, and HNA (all antibodies purchased from Abcam) by following standard protocols. The optical and fluorescent images were obtained using a light microscope (Olympus) and fluorescent microscope (Olympus), respectively. The cross-sectional area of myofibers, density of myofibers, and density of human cells in the muscle tissues were determined using ImageJ software (n = 3 mice, 10 randomly selected field from each mouse).

2.3.3. In vivo live imaging of injected cells

Before cell sheet detachment or treatment with trypsin, hUCBMSCs were labeled with DiO for 3 hr. At 4, 10, and 28 days after cell implantation into TA muscles, the mice were anesthetized with xylazine (10 mg/kg) and ketamine (100 mg/kg) and the retention of the injected cells was examined using an eXplore Optix System (Advanced Research Technologies Inc.).

2.4. Statistical analysis

All quantitative data are expressed as mean ± standard deviation. A one-way analysis of variance (ANOVA) using the Bonferroni test was performed to determine significant differences. The assumptions of ANOVA were found to satisfy Levene's test for homogeneity of variance and to pass tests for normality. A value of $p < 0.05$ was considered statistically significant.

Chapter 3.

A stretchable piezoelectric substrate providing pulsatile mechanoelectric cues for cardiomyogenic differentiation of mesenchymal stem cells

3.1. Introduction

MSC therapy is an attractive strategy for treating myocardial infarction, which causes cardiomyocyte loss and scar tissue formation resulting in the loss of regional contractility of the heart.[6, 33, 35-38] MSCs implanted into myocardial infarction regions exhibit therapeutic effects such as attenuating pathological cardiac remodeling and improving cardiac functions.[6, 36-37] However, it is generally accepted that MSCs implanted into cardiac infarction sites rarely differentiate into cardiomyocytes.[33] Therefore, the functional benefits observed in the MSC therapy for cardiac repair may be related to paracrine soluble factors secreted by the implanted MSCs rather than the differentiation of MSCs to cardiomyocytes.[39] Importantly, *ex vivo* induction of the cardiac phenotype in MSCs prior to implantation may further improve the efficacy of the MSC therapy for cardiac repair. Indeed, several studies have demonstrated that implantation of bone marrow-derived mesenchymal stem cells (BMSCs) that were induced to differentiate into cells with cardiomyocyte-like phenotypes *ex vivo* resulted in better cardiac tissue regeneration with larger improvement in cardiac function, than implanting non-modified BMSCs.[16, 38] Furthermore, in the previous study, the *ex vivo* modified BMSCs underwent myogenic differentiation after implantation, which is important for cardiac muscle regeneration and restoring contractility, but non-modified BMSCs did not.[16]

MSCs can exhibit cardiomyocyte-like phenotypes *ex vivo* by treatments with 5-azaC,[15, 40-41] growth factors such as TGF-β,[16] bFGF, IGF-1, BMP-2,[17] conditioned medium from cardiomyocyte culture,[18] and by co-culture with cardiomyocytes.[19, 42] However, although chemical factors, such as 5-azaC, are able to promote cardiomyogenic differentiation of MSCs, the efficiency is relatively low. Recently,

several studies have demonstrated that mimicking the microenvironments of *in vivo* cardiac tissue such as applying electric stimulation[24-25] or cyclic strain[26-27] (Fig. 3.1A), can enhance cardiomyogenic differentiation of MSCs more efficiently than chemical factors. However, no study has applied PMEC as a cardiac-mimetic microenvironments, in which mechanical strain (MS) and electric pulse (EP) are sequentially produced, to stimulate cardiomyogenic differentiation of MSCs *in vitro* yet.

Here, we developed a SPS that can provide PMEC to stimulate cardiomyogenic differentiation of human BMSCs *in vitro*. Piezoelectric materials can generate EP upon the deformation of their crystal structure by external MS.[43] Recently, piezoelectric materials have been applied to many fields including self-powered devices,[44] liquid crystal displays,[45] and medical devices.[46-47] The SPS used in this study was designed in the form of multi-stacked layer-by-layer composite consisting of aligned ZnO NRs and PDMS. Unlike typical uni-axial grown ZnO NR, bi-axially grown ZnO NR has been reported as a highly efficient piezoelectric crystal which can generate EP upon its c-axis bending.[48] Moreover, the ZnO NR is biocompatible[49] enough to be selected as the piezoelectric material in this study.

The SPS was used as a culture substrate for hMSCs to stimulate cardiomyogenic differentiation *in vitro* by providing the PMEC (Fig. 3.1B), which mimics the *in vivo* cardiac microenvironments. We have stimulated hMSCs for 10 days for cardiomyogenic differentiation, because previous studies used one or two weeks to induce cardiomyogenic differentiation of MSCs.[14, 41]

Using a custom-made culture chamber (Fig. 3.1C) we subjected the SPS to cyclic bending and stretching, which generated cyclic EP and MS. According to a previous study, cells can be stimulated by non-contact electric field when the cells

are cultured on an insulating material that is placed on an electric field generator.[26] This is attributed to that electric field or electrostatic potential is formed on the insulating material surface when electric potential differences are present.[50] Although PDMS is an insulating material, it has a low dielectric constant (≈ 2.3),[51] indicating that PDMS of the SPS can be electrically charged by the electrical potential differences upon bending the SPS. Thus, bending the SPS can electrically stimulate hMSCs cultured on the SPS, even though the piezoelectric ZnO NRs of the SPS are wrapped with insulating PDMS. Finally, we investigated whether our technique stimulated cardiomyogenic differentiation of MSCs and cellular signaling pathways related to cardiomyogenic differentiation.

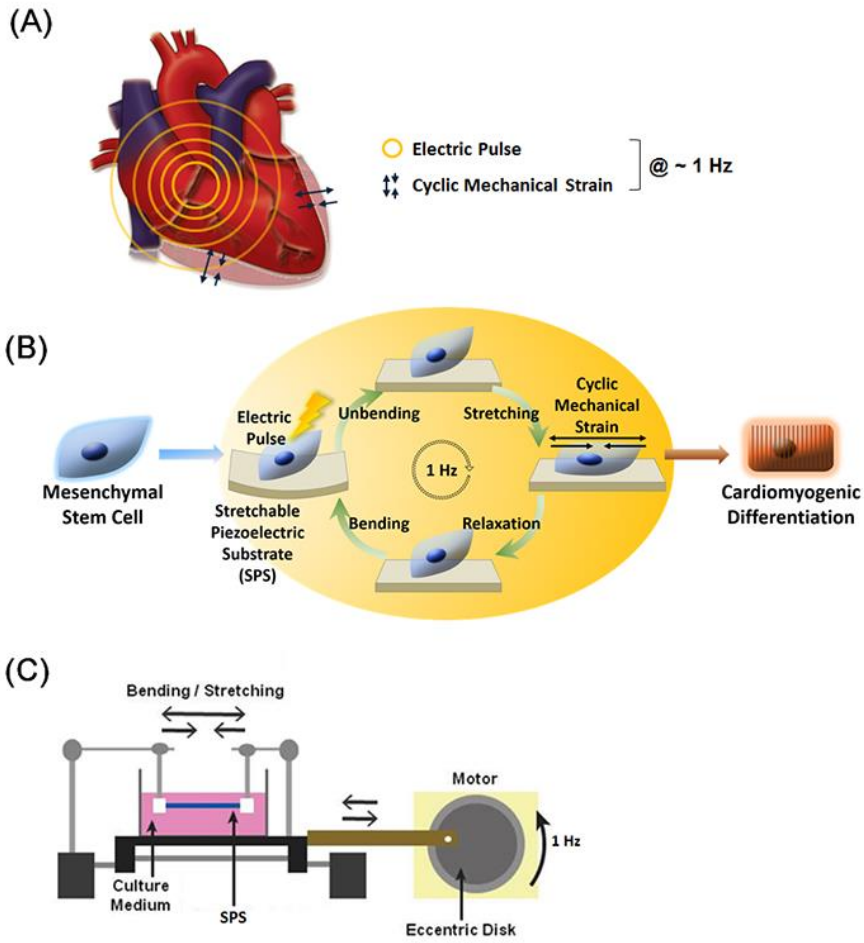

Figure 3.1. Schematic diagrams for stimulation of cardiomyogenic differentiation of hMSCs using stretchable piezoelectric substrate (SPS). (A) Electric pulse and cyclic mechanical strain signals are present in cardiac microenvironments. (B) SPS, on which hMSCs are cultured, can mimic the cardiac microenvironments and generate electric pulse and cyclic mechanical strain signals upon bending and cyclic stretching, respectively, to stimulate cardiomyogenic differentiation of the hMSCs. (C) The custom-made cell culture chamber to subject the SPS, on which hMSCs were cultured, to cyclic bending and cyclic stretching.

3.2. Results and discussion

3.2.1. Piezoelectric characteristics of SPS

Figure 3.2A shows a typical process for fabricating SPS, which is based on a previous study.[48] ZnO NR powder was produced using a kinetically controlled wet chemical method.[34] The ZnO NRs were placed on a PDMS substrate and rubbed against another PDMS block in one direction. This created a monolayer of the ZnO NRs that were aligned in the direction of rubbing (Fig. 3.2B). During rubbing, one prismatic side (Fig. 3.2C) of ZnO NRs was affixed to the hydrophobic surface of the PDMS substrate along its in-plane direction until the entire surface of the substrate was covered with ZnO NRs. Strong van der Waals forces allowed the ZnO NRs to attach to the PDMS substrate. We then coated this monolayer with another thin PDMS layer to fasten the ZnO NRs to the substrate, thus forming the first layer of the NRs. By repeating this procedure five times, a multi-layered SPS was fabricated (Fig. 3.2A). The number of ZnO NR monolayers in the SPS was selected to generate a proper output voltage for electrically stimulating hMSCs.

In order to evaluate the output voltage and current density generated on the surface of the SPS upon bending, an energy-harvesting device with five layers of piezoelectric ZnO NRs was fabricated. The energy-harvester, of which the top and bottom sides of SPS was deposited with silver electrodes, was put on a PDMS substrate having the same thickness of the SPS and activated with a 20-mm bending radius. When the device was convexly bent, a positive voltage and current density were generated (Fig. 3.2D and F). Upon releasing the bending stress, a negative voltage and current density were produced. The five-layered SPS generated 3 V (Fig. 3.2D). This voltage represents the electric potential difference between the top

and bottom sides of the device, which were +1.5 V and -1.5 V, respectively. Additionally, to prove the piezoelectric behavior of the SPS, polarity changes in the voltage and current density produced in the SPS were measured using a reverse connecting method as shown in figure 3.2E and G. When the electrical connecting direction was reversed, the polarities of the voltage and current density on the top side became negative.

The surface charge density of the SPS containing ZnO NRs is changed by bending the SPS, since the permanent dipole moment of each ZnO NR has the time-dependent deviation during the bending. PDMS of the SPS has no permanent dipole moment but finite dielectric property (dielectric constant $\approx$ 2.3).[51] Thus, the electrostatic potential generated by the deviation in dipole moment of the ZnO NRs can be transferred to the surface of the SPS by charging the capacitance of the PDMS. Until fully charging the capacitance, the surface charge density of the SPS would be changed. Based on this principle, periodically changing surface charge density is generated on the surface of the SPS by the cyclic bending motion (Fig. 3.2D-G). Thus, hMSCs cultured on the SPS can be electrically stimulated by cyclic bending

The alignment of ZnO NRs in SPS was examined by optical microscopy. The direction of ZnO NRs was quantified at day 0 and after 10 days of cyclic bending and stretching. No significant change in the alignment of ZnO NRs was found for 10 days (Fig. 3.2H), so it could be assumed that the electric property of SPS would be maintained at least for 10 days of cell culture. In addition, SPS exhibited elastic properties over 10 days of bending/stretching due to the elasticity of PDMS (Fig. 3.2I). The length of the SPS did not change over 10 days of bending/stretching compared to the original length.

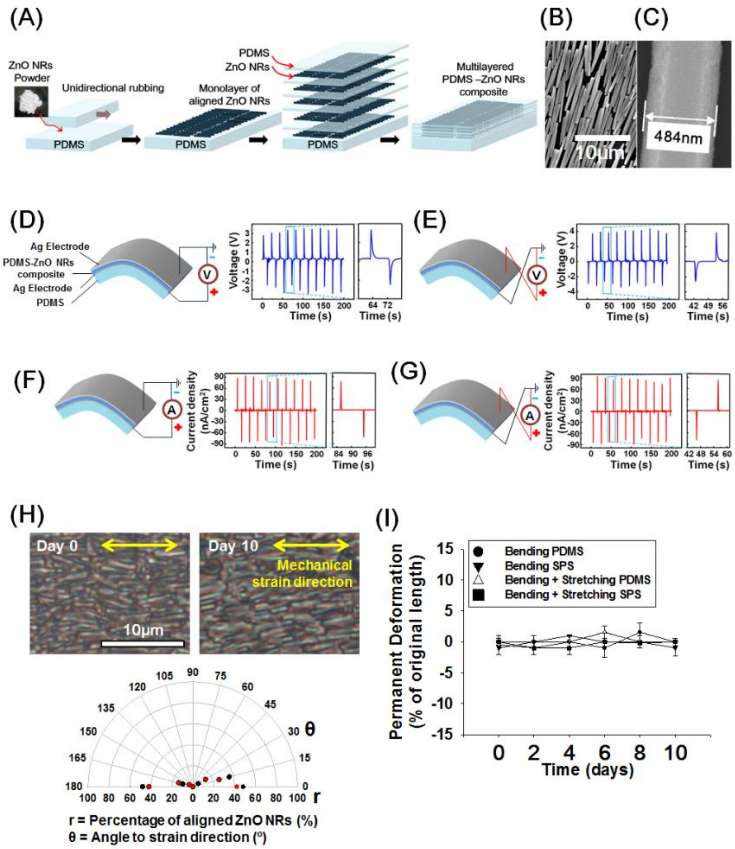

Figure 3.2. Fabrication and characterization of SPS. (A) The fabrication process of SPS. SEM images of (B) aligned zinc oxide nanorods and (C) single zinc oxide nanorod in the SPS. Open circuit voltages generated on the SPS surface connected in the (D) forward and (E) reverse directions. Short circuit current density generated from the SPS connected in the (F) forward and (G) reverse directions. (H) Alignment of ZnO NRs in SPS at day 0 and after 10 days of cyclic bending and stretching. ZnO NRs were visible under light microscopy as the ZnO NR layer was covered by a very thin layer of PDMS. The orientations of ZnO NRs were quantified on day 0 (black) and after 10 days (red) of cyclic bending and stretching. (I) Permanent deformation profiles of SPS and PDMS subjected to either cyclic bending or cyclic bending/cyclic stretching for 10 days. SPS length = 5 cm. Bending radius = 20 mm. Amplitude of cyclic stretching = 3 % of original SPS length.

3.2.2. Cytotoxicity of SPS, bending, stretching, and EP

Prior to cell differentiation experiments, the cytotoxicity of SPS, bending, stretching, and EP was evaluated by culturing hMSCs on SPS with or without stimulation. The biocompatibility and biosafety of ZnO nanowires were evaluated in a previous study, and showed no cytotoxicity below a concentration of 100 μg/ml.[49]

PDMS, ZnO NRs, and 5-azaC are known to be non-cytotoxic, however, we had to observe the apoptotic effects of EP and MS, especially at 3 V and 3 % of magnitude, respectively, as the EP and MS stimulation could induce apoptosis of hMSCs.

The SPSs were bent and unbent at a 20-mm bending radius to generate bi-polar pulsed 3 V EP. The SPSs were also subjected to cyclic strain at 3 % of the original length. The cytotoxic effect was evaluated by immunofluorescence staining of caspase-3, an apoptotic marker (Fig. 3.3A), and RT-PCR of *CASPASE-3* (Fig. 3.3B), B-cell CLL/lymphoma 2 (*BCL-2*, anti-apoptotic marker), and *P53* (pro-apoptotic marker) (Fig. 3.3C). The results showed that no cytotoxic effect was induced by SPS itself, EP generated by SPS bending, cyclic bending (of PDMS), and stretching.

The cells in first group is the hMSCs cultured on tissue culture plate, as a negative control for cardiomyogenic differentiation. The cells of second and third group were cultured on PDMS and SPS, respectively, without external stimulation such as EP or MS. The cells of forth group were cultured on PDMS and were cyclic bent, to evaluate the effect of the bending motion of the substrate. The cells of fifth group were cultured on SPS and cyclic bent, to be electrically stimulated by EP

generation. The cells in sixth group were cultured on PDMS, and were cyclic bent and stretched, to be mechanically stimulated. The cells in last group were cultured on SPS, and were cyclic bent and stretched, to be simultaneously stimulated by MS and EP.

A previous study used 10 V electrostimulation for inducing cardiomyogenic differentiation of MSCs.[25] In contrast, we used 3 V to circumvent the possible harmful apoptotic effects of EP on hMSCs as electrical stimulation above 10 V can decrease the viability of the cells.[52] Previous studies have used a stretching amplitude of 10 % of the original length to induce cardiomyogenic or vascular differentiation of MSCs.[27, 53] However, more than 5 % of stretching amplitude induced cell detachment and even cell death in the present study (data not shown). Therefore, we used 3 % of stretching amplitude of in this study, which showed no cytotoxicity or cell detachment but able to induce cell alignment.

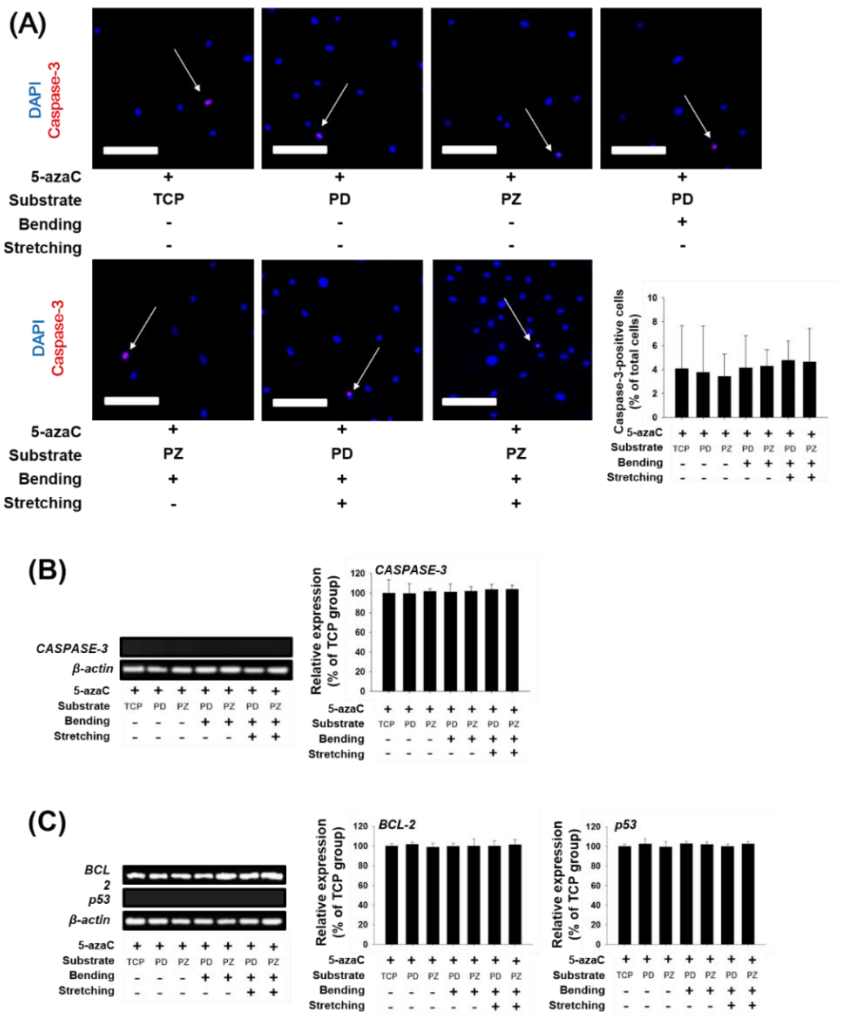

Figure 3.3. Cytotoxicity of SPS, bending, CS, and EP. (A) Apoptotic activity of hMSCs cultured under various conditions for 10 days as evaluated by immunocytochemistry for caspase-3 (red, arrows, n = 3 per group). Blue indicates nucleus (DAPI). Scale bars indicate 100 μm. TCP, PD and PZ stand for tissue culture plate, PDMS and SPS, respectively. (B, C) RT-PCR analyses of hMSCs cultured under various conditions for 10 days for detecting pro- (CASPASE-3 and p53) and anti-apoptotic (BCL-2) gene expression, and quantification relative to the TCP group (n = 4 per group).

3.2.3. Cell alignment induced by cyclic stretching

Cardiac cell alignment is important for anisotropic action potential propagation and cardiac contraction.[54] MSCs are known to align perpendicularly to the direction of cyclic stretching to minimize the external stress.[27] F-actin staining analysis revealed that cyclic stretching induced a perpendicular alignment of hMSCs (Fig. 3.4), which is in accordance with the results of previous studies,[27, 53] while cells randomly aligned in the other groups. Bending or EP did not induce cell alignment. cyclic stretching also enhanced the expression of Cx43 (Fig 3.5A), a protein strongly related to cell-cell coupling and cellular conductivity, which are essential to the cardiac contraction.[54] The cyclic stretching-induced cell alignment and Cx43 expression is in agreement with the results of previous reports in which cardiomyocytes and smooth muscle cells subjected to cyclic stretching were aligned and expressed more Cx43.[55-56]

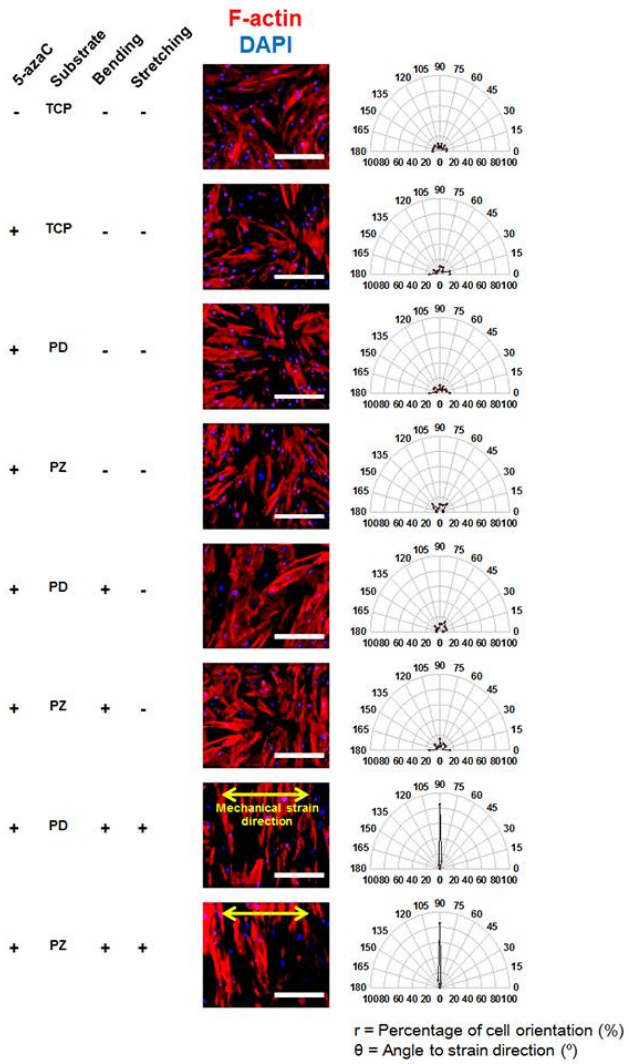

Figure 3.4. hMSC alignment induced by cyclic stretching for 10 days, as evaluated by F-actin staining (phalloidin staining, red). Blue (DAPI) indicates the nucleus of hMSC. Scale bars indicate 30 μm. Cyclic stretching induced hMSC alignment perpendicular to the cyclic stretching direction. Bending and EP did not induce cell alignment. Cell alignment was quantified by determining the angles of F-actin-stained cells to the cyclic strain direction (n = 4 per group). TCP, PD and PZ stand for tissue culture plate, PDMS and SPS, respectively.

3.2.4. Enhanced cardiomyogenic differentiation by EP and cyclic stretching.

We investigated whether EP and cyclic stretching additively promote the cardiomyogenic differentiation of hMSCs (Fig. 3.5). Treatment with 5-azaC induced the expression of cardiomyogenic genes at low levels, which is in accordance to previous studies.[14-15, 38] After treatment with 5-azaC (i.e., under permissive condition for cardiomyogenic differentiation), EP and cyclic stretching additively promoted the expression of early stage cardiac markers, such as cardiac-associated transcription factors [NK2 homeobox 5 (NKX2.5), myocyte enhancer factor 2 (MEF-2), and GATA binding protein 4 (GATA4)], late stage cardiac-specific structural markers, such as beta myosin heavy chain (β-MHC) and sarcomeric α-actinin,[28] and a gap junction protein (Cx43), as evaluated by Western blot analyses (Fig. 3.5A). In the absence of bending and CS, PDMS and SPS groups did not exhibit enhanced cardiomyogenic differentiation. The enhanced expression of Cx43 and sarcomeric α-actinin in the EP and cyclic stretching group was confirmed by immunocytochemistry (Fig. 3.5B). In the cardiac microenvironment, gap junction proteins (Cx43) are essential for the conductivity between cells (i.e., cell-to-cell calcium ion fluctuation) and contraction of the cells.[54, 57-59] Previous studies have shown that cardiomyocytes express more Cx43 when subjected to cyclic stretching.[55, 60] Cardiomyogenic differentiation of MSCs induced by either EP or cyclic stretching has already been reported in previous studies.[24-25, 27, 61] However, no study has reported the additive enhancement in cardiomyogenic differentiation of MSCs by EP and cyclic stretching, so far. Additionally, EP and cyclic stretching additively promoted mRNA expressions of ion channel markers, such as cyclic nucleotide-gated potassium channel 2 (*HCN2*) and calcium channel,

voltage-dependent, L type, alpha 1C subunit (*CACNA1C*), as evaluated by qPCR (Fig. 3.5C). The ion channels are known to be essential for the electrical activity of the heart such as the generation of ion currents for action potential.[62] Meanwhile, contraction is one of the critical functions of mature cardiomyocytes, and some studies have observed the contractility of cardiomyogenic cells, especially differentiated from embryonic stem cells or induced pluripotent stem cells. However, many studies observed that cardiomyogenic cells differentiated from MSCs did not show cell contraction. In agreement of those studies, we had not observed the contractility of the cardiomyogenic cells differentiated cells from hMSCs.

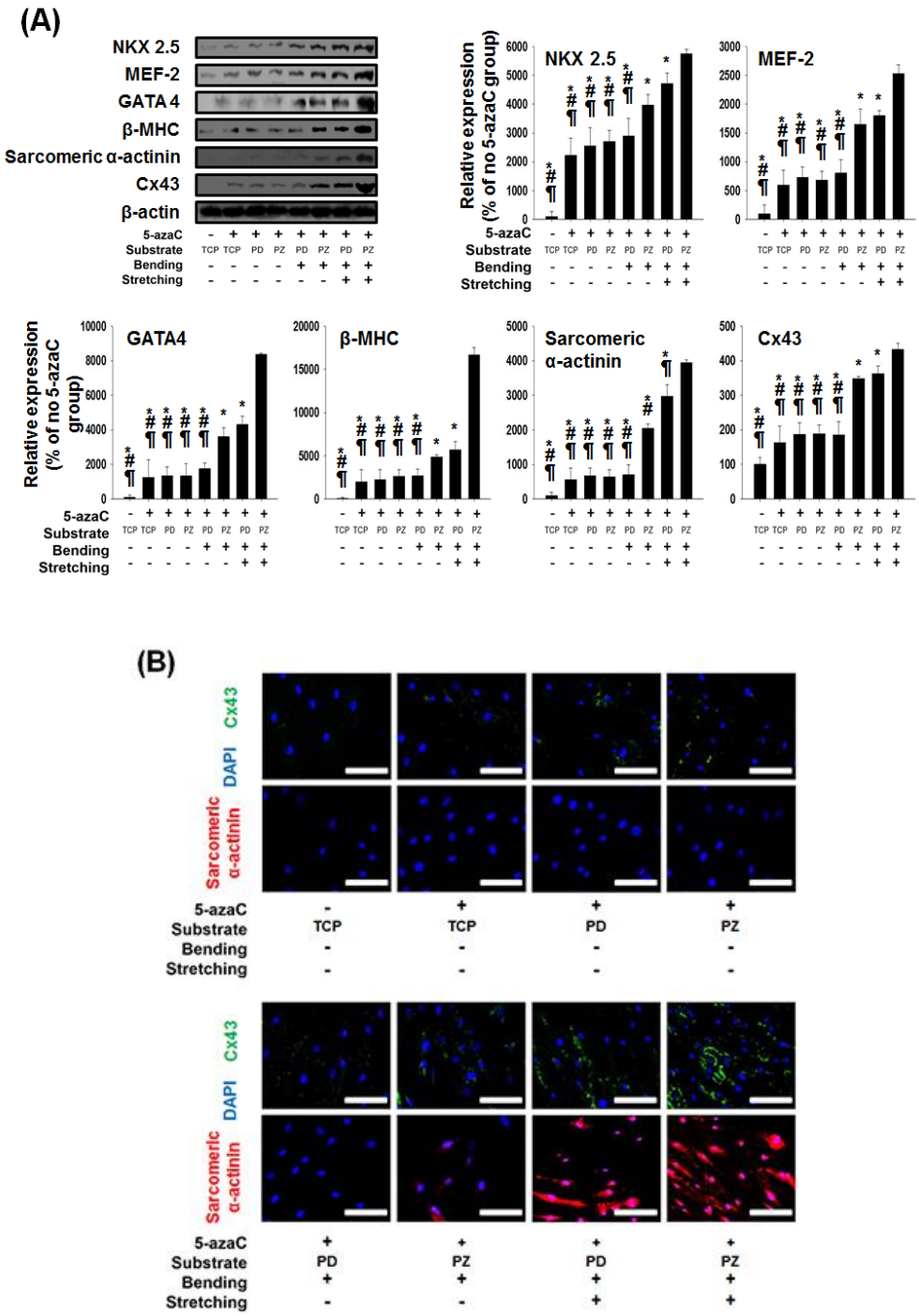
(A)
NKX 2.5
MEF-2
GATA 4
β-MHC
Sarcomeric α-actinin
Cx43
β-actin
5-azaC
Substrate
Bending
Stretching
TCP TCP PD PZ PD PZ PD PZ
Relative expression (% of no 5-azaC group)
NKX 2.5
MEF-2
GATA4
β-MHC
Sarcomeric α-actinin
Cx43
(B)
Cx43
DAPI
Sarcomeric α-actinin
5-azaC
Substrate
Bending
Stretching
TCP
PD
PZ

Figure 3.5.A-B.

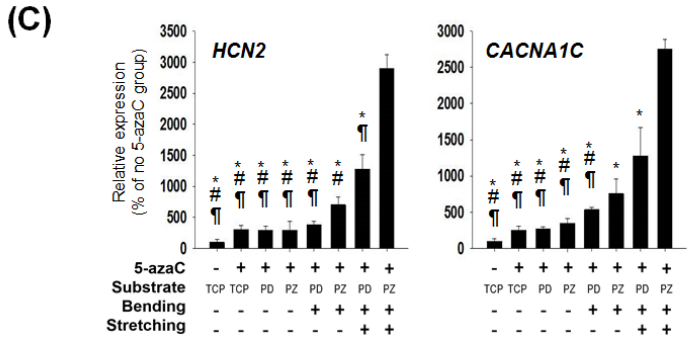

Figure 3.5. Enhanced cardiomyogenic differentiation of hMSCs *in vitro* by EP and cyclic stretching for 10 days. (A) Western blot analysis and quantification for early (NKX 2.5, MEF-2, and GATA4) and late stage (β-MHC and sarcomeric α-actinin) cardiac markers, and Cx43. (n = 4 per group, *p < 0.05 versus the PZ/bending/stretching group, #p < 0.05 versus the PDMS/ bending/stretcing group, ¶p < 0.05 versus the PZ/bending group). (B) Enhanced expression of Cx43 (green) and sarcomeric α-actinin (red) as evaluated by immunocytochemistry. Blue (DAPI) indicates the nucleus of hMSC. Scale bars indicate 50 μm. (C) mRNA expression of ion channel markers (HCN2, CACNA1C) as quantified by qRT-PCR. (n = 4 per group, *p < 0.05 versus the PZ/bending/stretching group, #p < 0.05 versus the PDMS/bending/stretching group, ¶p < 0.05 versus the PZ/bending group) TCP, PD and PZ stand for tissue culture plate, PDMS and SPS, respectively.

3.2.5. Cardiomyogenic differentiation-related autocrine growth factor expression and intracellular signaling enhanced by EP and cyclic stretching.

Figure 3.6A summarizes autocrine factor expression and intracellular signaling pathways, which can be stimulated by EP and cyclic stretching, for cardiomyogenic differentiation of MSCs. EP or electric field is known to increase the expression of growth factors,[63] such as BMP-4,[64] IGF,[65] vascular endothelial growth factor (VEGF),[66] and TGF-β,[65] that enhance the cardiomyogenic differentiation of MSCs in an autocrine mechanism. Cyclic stretching is known to increase the expression of IGF,[67] VEGF,[68-69] and TGF-β.[70-71] BMP-4 is known to induce cardiomyogenic differentiation by enhancing phosphorylation of SMAD-1,4,5,8 and upregulating NKX2.5, MEF-2, and β–MHC.[72-73] VEGF and TGF-β were shown to enhance Cx43 expression.[74] IGF was shown to induce cardiomyogenesis by enhancing phosphorylation of *p38* and upregulating MEF-2.[75] As demonstrated by RT-PCR data in figure 3.6B, EP and cyclic stretching additively upregulated mRNA expression of BMP-4, TGF-β, VEGF, and IGF in hMSCs, which are autocrine factors that enhance cardiomyogenic differentiation via the intracellular signaling mechanism shown in figure 3.6A. As hMSCs were stimulated by the autocrine factors, EP and cyclic stretching additively enhanced the protein expressions of intracellular signaling molecules for cardiomyogenic differentiation [phosphorylated p38 (pp38) and phosphorylated SMAD (pSMAD)], as evaluated by Western blot analyses (Fig. 3.6C). Additionally, the phosphorylation of focal adhesion kinase (FAK) and extracellular signal-regulated kinases 1/2 (ERK1/2) are known to be enhanced by electric stimulation[76-78] and cyclic stretching.[79] The phosphorylation of ERK1/2 upregulates cardiomyogenic differentiation by

elevating GATA4 expression.[80] As all data were quantified, the relative expressions of phosphorylated p38 (pp38), phosphorylated SMAD (pSMAD), pFAK, and pERK1/2 compared to p38, SMAD, FAK, ERK1/2, respectively, were additively enhanced by simultaneous EP and cyclic stretching signals, compared to the hMSCs stimulated by either EP or cyclic stretching (Fig. 3.6C).

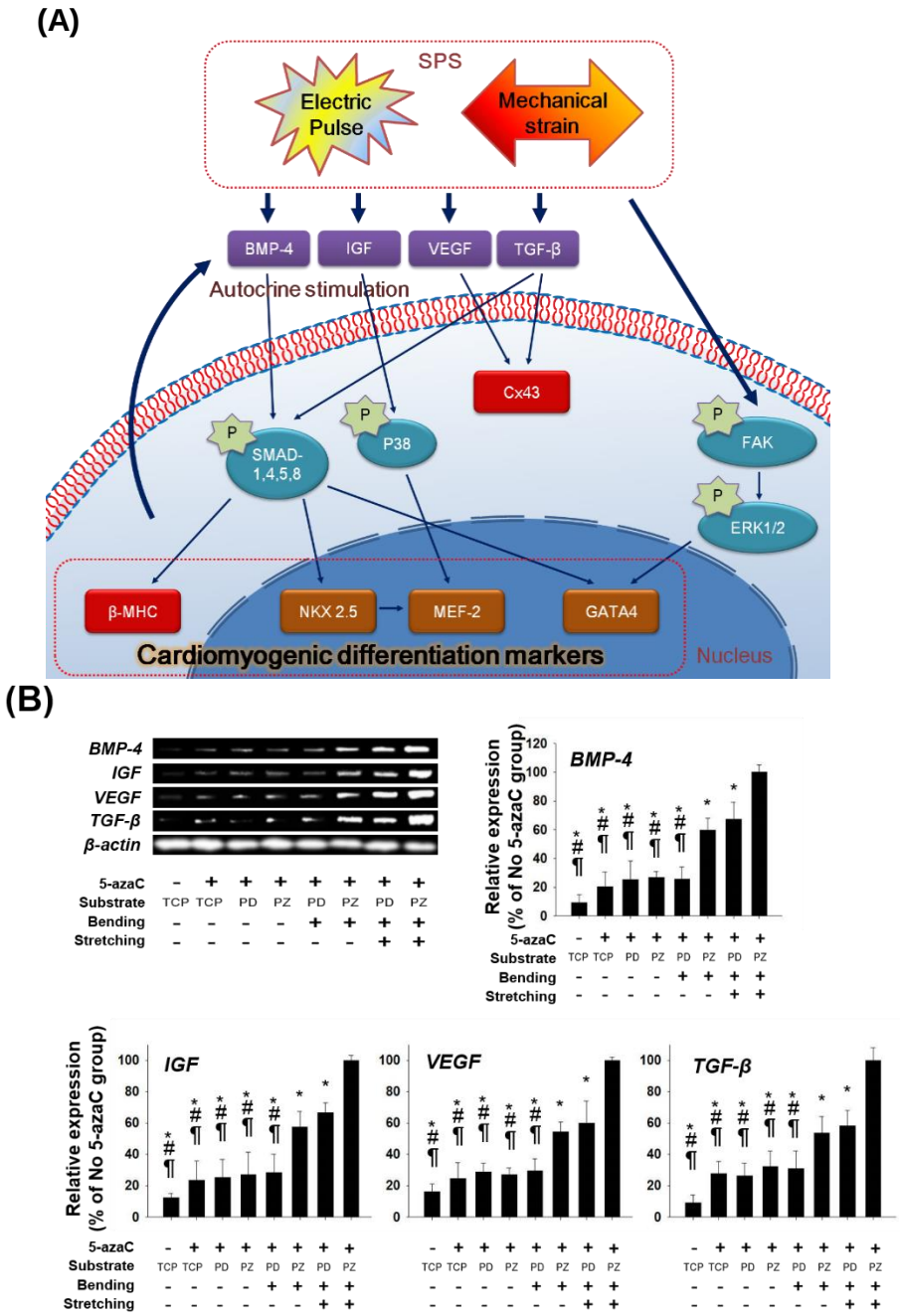
(A)
SPS
Electric Pulse
Mechanical strain
BMP-4
IGF
VEGF
TGF-β
Autocrine stimulation
Cx43
P
SMAD-1,4,5,8
P38
FAK
ERK1/2
β-MHC
NKX 2.5
MEF-2
GATA4
Cardiomyogenic differentiation markers
Nucleus
(B)
BMP-4
IGF
VEGF
TGF-β
β-actin
5-azaC
Substrate
Bending
Stretching
TCP
PD
PZ
Relative expression (% of No 5-azaC group)

Figure 3.6.A-B.

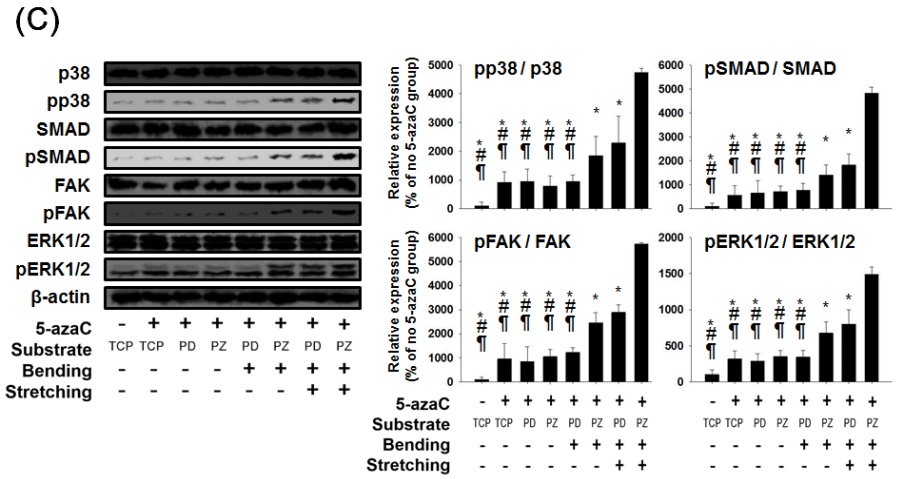

Figure 3.6. Cardiomyogenic differentiation-related autocrine factor expression and intracellular signaling enhanced by EP and cyclic stretching. (A) A schematic diagram describing autocrine growth factor expression and intracellular signaling pathways for cardiomyogenic differentiation of MSCs enhanced by EP and cyclic stretching. (B) mRNA expression of autocrine growth factors (BMP-4, TGF-β, VEGF, and IGF) on 10 days as evaluated by RT-PCR (n = 4 per group, *p < 0.05 versus the PZ/bending/stretching group, #p < 0.05 versus the PDMS/bending/stretching group, ¶p < 0.05 versus the PZ/bending group). (C) Protein expressions of intracellular signaling molecules for cardiomyogenic differentiation on 10 days, as evaluated by western blot analyses. (n = 4 per group, *p < 0.05 versus the PZ/bending/stretching group, #p < 0.05 versus the PDMS/bending/stretching group, ¶p < 0.05 versus the PZ/bending group). TCP, PD and PZ stand for tissue culture plate, PDMS and SPS, respectively.

Chapter 4.

Thermosensitive, stretchable, and piezoelectric substrate for generation of myogenic cell sheet fragments from human mesenchymal stem cells

4.1. Introduction

Sarcopenia**,** which is a skeletal muscle disease associated with aging, is the degenerative decline of skeletal muscle mass and strength. The disease causes severe social problems and reduction in quality of human life. Once a skeletal muscle tissue is damaged, the satellite cells, the skeletal muscle precursor cells that reside in skeletal muscle, start to proliferate, migrate, and differentiate for myogenesis.[81-82] In the process of myogenesis, several cellular events are observed; expression of myogenic regulatory factors (MRFs) including MyoD, Myf5, Myf6, and Myogenin, cell alignment and cell fusion.[83] However, the muscle loss with aging is likely caused by the decrease in the number and myogenic differentiation capability of the muscle satellite cells.[84] Thus, implantation of myogenic differentiated cells may be necessary to treat such muscle disorder.

MSCs have a great potential for treating skeletal muscle diseases, by secretion of paracrine factors[85] or by differentiating into muscle cells to be part of the host myofiber.[86] It has been known that MSCs derived from various sources can differentiate into muscle cells.[21, 87-88] In particular, hUCBMSCs have advantages for skeletal muscle regeneration because they are able to differentiate into myocytes and easy to obtain in large quantities for allogenic or autogenic implantation or secrete paracrine factors.[89-90] Autologous MSCs derived from aged patients' bone marrow or adipose tissues may not be ideal stem cells for skeletal muscle because MSCs isolated from aged humans have limited capability of proliferation and differentiation.[91] Several approaches have been attempted to induce myogenic differentiation of stem cells; development of myogenic medium,[20-21] culturing cells

in three-dimensional scaffold,[22] modulating matrix stiffness[13,15] and expose to laser irradiation.[23]

Recently, several studies have tried to mimic *in vitro* either the electrical[92-93] or mechanical[94] properties of native muscle. Subjecting cells to electrical and mechanical stimulation mimics the physiological environment of native skeletal muscle, as the muscle cells mechanically contract by action potential stimulation from motor neurons (Fig. 4.1A). However, there has not yet been any research to simultaneously apply both electrical and mechanical stimulation for myogenic differentiation of stem cells *in vitro*. To provide both electrical and mechanical stimulation for myogenic differentiation of hUCBMSCs, here we developed a thermosensitive, stretchable, and piezoelectric substrate (TSPS). TSPS is composed of three parts; (i) aligned bi-axially grown ZnO NRs to provide piezoelectric pulse (PP) which is produced by cyclic bending of TSPS, (ii) polydimethylsiloxane (PDMS) that can be stretched by external force to provide mechanical strain (MS), and (iii) thermosensitive poly(N-isopropylacrylamide) (pNIPAAm) which is coated on the PDMS surface and forces the cells to be detached from TSPS at a low temperature. ZnO NRs, which have a piezoelectric property, in TSPS were bi-axially grown unlike typical uni-axial grown ZnO NRs to generate PP upon its c-axis bending,[48] and are biocompatible.[49] TSPS was repetitively bent and stretched for 10 days at 0.3 Hz in a custom-designed cell culture chamber, providing PMEC to attached hUCBMSCs to produce myogenic differentiated cell sheets from hUCBMSCs (Fig. 4.1B). To detach the cells as cell sheets, TSPS was cooled down to 4 ℃. The detached cell sheets were spliced into small fragments for injection into CTX-induced skeletal muscle injured mice. Generation of myogenic differentiated cell sheet fragments from hUCBMSCs using TSPS, which mimics

the native skeletal muscle microenvironment, may be a promising stem cell therapy to treat muscular diseases.

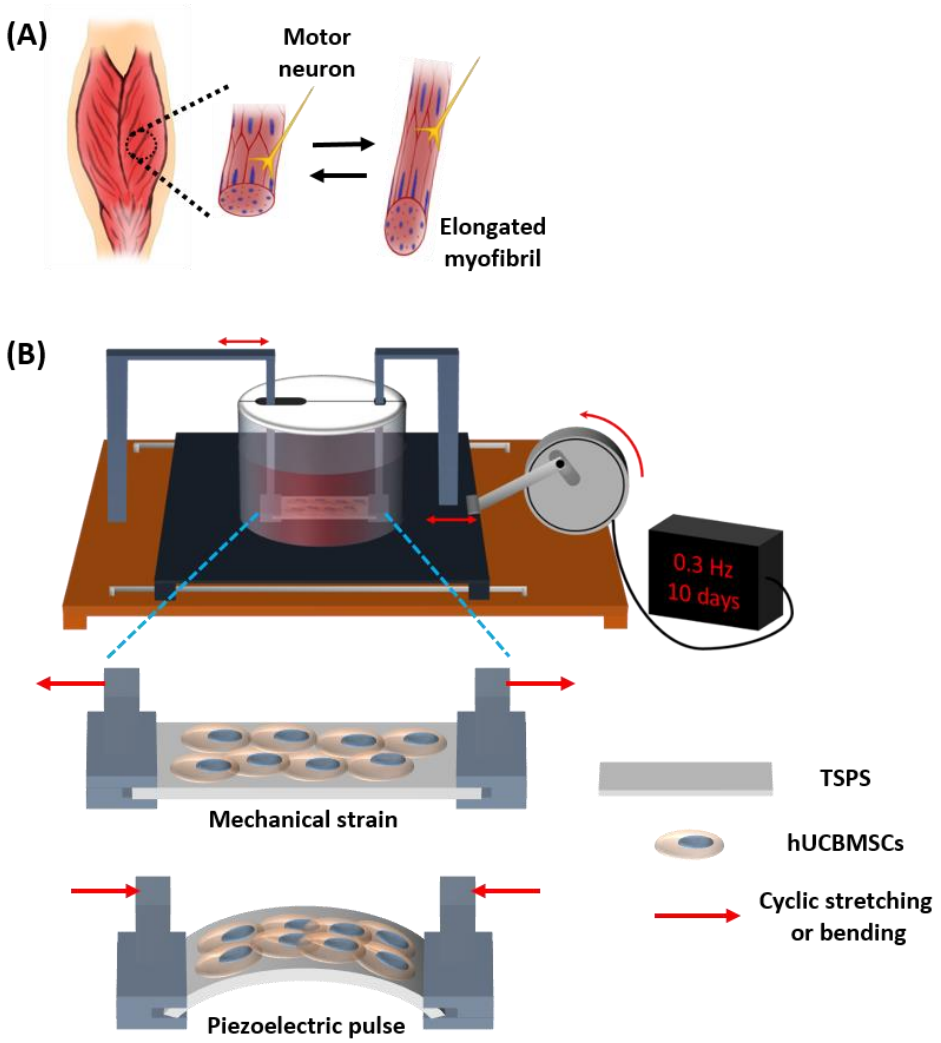

Figure 4.1. Schematic diagrams for myogenic differentiation of hUCBMSCs using TSPS. (A) Mechanical and electrical stimulation in native skeletal muscle microenvironment, which is mimicked in the present study for myogenic differentiation of hUCBMSCs *in vitro*. (B) A custom-designed cell culture chamber to provide mechanical and electrical stimulation to hUCBMSCs cultured on TSPS for myogenic differentiation. Cyclid bending and stretching of TSPS were repeated at 0.3 Hz for10 days.

4.2. Results and discussion

4.2.1. Piezoelectric characteristics of TSPS

The shape of bi-axially grown-ZnO NRs is shown in figure 4.2A. The hexagonal pillars were grown in the [0001] direction mirror-symmetrically with respect to the center plane. The length of ZnO NR was about 3.5 μm. The diameter was about 500 nm at the center and 400 nm at the end. A monolayer layer of aligned ZnO NRs (Fig. 4.2B) was obtained through a one-directional dry rubbing process. Almost all ZnO NRs are aligned in the direction of rubbing. Our TSPS consists of three layers of aligned ZnO NRs and multistacked PDMS (Fig. 4.2C). The thickness of each layer PDMS was 5 μm and the thickness of the rear substrate PDMS was 3 mm. A device was fabricated as shown in figure 4.2D to evaluate the PP generation characteristics of TSPS due to the bending of TSPS. As a flexible electrode suitable for bending deformation, composite electrode combined silver nanowire (70%) with single-walled carbon nanotubes (SWCNT) (30%) was used. The PP generated from TSPS by repetitive deformation with a bending radius of 36 mm is shown in figure 4.2E. The bending cycle was 0.3 Hz. The average peak-to-peak potential was designed to be 120 mV (Fig. 4.2E), being a similar level to the change of cell membrane potential caused by action potential, to mimic the native muscle microenvironment.[95]

In order to investigate the mechanism of piezoelectric phenomena of ZnO NRs by nonlinear bending deformation, the theoretical calculation of piezoelectric potential generation from ZnO NRs inside PDMS was performed using COMSOL Multiphysics® . Considering the deformation direction due to bending and the direction of the piezoelectric polarization, it can be expected that the piezoelectric

material's flexoelectric term μ_{31} mode is dominant. Based on this hypothesis, ZnO NR, a symmetrical hexagonal column wedge with a length of 3.7 μm and a diameter of 600 nm at both ends and 400 nm at both ends was used in the model. Two ZnO crystal regions with opposite c-axis crystal orientations with respect to the center plane were set up, and three layers with ZnO NRs aligned in the middle of 5 μm PDMS were stacked. The bending curvature of 36 mm was applied and the resulting PP distribution is shown in figure 4.2C. The negative potential in the direction of the bending center represents the positive potential in the opposite direction, and the magnitude of the potential difference between top and bottom side was similar to that measured in the experiment. From this result, we could confirm that the piezoelectric potential occurs from the μ_{31} mode of ZnO NRs used in this work.

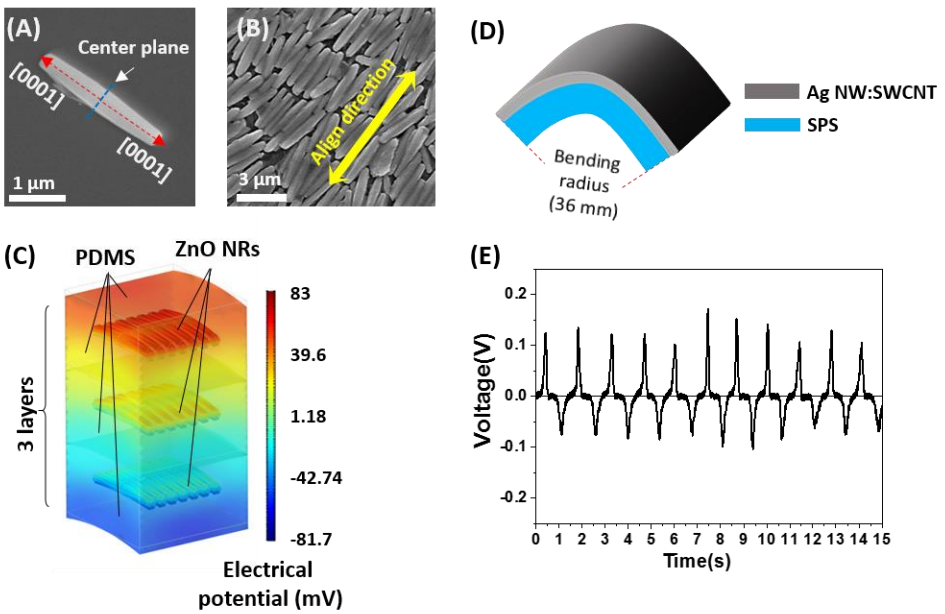

Figure 4.2. Fabrication and piezoelectric charisteristics of TSPS. (A) A single crystalline ZnO NR. (B) A monolayer of one-directionally aligned ZnO NRs. (C) The piezoelectric potential distribution in TSPS consisting of three layers of ZnO NRs (bending radius 36 mm) as calculated by COMSOL Multiphysics® . (D) Schematic configuration of TSPS at bending radius 36 mm. (E) Piezoelectric potentials generated from TSPS under repetitive bending.

4.2.2. Simulation of the electrical effects of TSPS on hUCBMSCs

Predicting the electric potential generated from TSPS to be transferred to the cell membrane is of great significance in interpreting the cell differentiation results by electrical stimulation.[96-98] Since the PP results in figure 4.2 are measured in air, not in cell culture medium, an additional consideration is needed to calculate the electrical potential transferred to the cell membrane (CM) (V_{mem}). Actually, the electrodes have been omitted from the structure of the TSPS used for cell culture. Since TSPS is fully submerged inside the cell culture medium, we can consider a closed circuit between both sides of the TSPS and the medium. In TSPS, there is a 3-mm thick PDMS dielectric layer in the lower part compared to the upper part of 5 μm, the potential transfer to the lower surface is hardly achieved. Therefore, it is assumed that the transferred potential at the bottom side of TSPS is close to zero. Also, it is assumed that there is almost no potential difference between the electrical double layer (EDL) layer between the lower surface of the TSPS and the cell culture medium. Considering electric conductivity (1.6 S/m) of the cell culture medium, it is assumed that the potential of the cell culture medium surrounding the patch is the same. Finally, the potential difference between cell culture medium and cell interior is fixed at -70 mV, which corresponds to the potential of the resting membrane of most cells.

Under the mentioned assumptions, the potential at the top of the patch is set to be a function of peak-to-peak of 60 mV, which is half value of measured voltage signal. The theoretical voltage wave changing over time every 3 s, is shown in figure 4.3A.

$$V(t) = 0.06\exp[-\frac{1}{2}(\frac{t-0.8}{0.15})^2] \ \ (0 < t < 1.6s)$$

$$V(t) = -0.06\exp[-\frac{1}{2}(\frac{t-2.4}{0.15})^2] \ \ (1.6s < t < 3.2s)$$

The detailed mathematical representation was shown above. Three EDL layers, one CM, and extracellular matrix (ECM) were considered as shown in figure 4.3B to predict the potential transfer to the CM of growing cells on the patch of interest in this study. The potential generated from the patch was applied to the lower EDL of the ECM and the potential for transfer of the potential through the impedance of each layer to the CM was calculated as a function of time through COMSOL Multiphysics®. To calculate the potential value transferred to cell membrane from TSPS, the properties of EDL and CM were quoted from known values. The thickness of EDLs were set to 2 nm, and the dielectric constant were set to 3.2.[99] The thickness of CM was set to 5 nm, and the dielectric constant was set to 2.3. [100-101] However, ECM is soaked in cell culture media, and its impedance has to be calculated based on the porosity and thickness of ECM. The thickness was roughly set to 100 nm, as an average value of several researches.[102-103] The porosity of ECM was set to 93.3 %.[104] The dielectric constant of cell culture media was set to 80,[105] and that of ECM, assuming that ECM is fully composed of collagen, was set to 4.5.[106] As a result, the net dielectric constant of the ECM layer is calculated and was set to 82.3, by combining these three values. The overall model was set to 100 μm in diameter. (Fig. 4.3E)

The results of the potential distribution over the model geometry at 0.8 s and 2.4 s with the greatest potential delivered from the patch is shown in figure 4.3C. Since the intracellular potential is fixed at -70 mV, the potential at both sides of the CM at 0.8 s, which is the maximum positive applied potential, is the highest, whereas at 2.4 s, which is the maximum negative applied potential, is the lowest. To determine the magnitude of potential at each layer during one period of applied

voltage waveform, the potential distribution over time in line A-A 'of figure 4.3B was calculated and the result is shown in figure 4.3D. The value of V_{mem} in this study was estimated to be -8 mV maximum and -64 mV minimum, which is similar to that of depolarizing and repolarizing cells.[95] Such changes in V_{mem} may cause the increase of intracellular calcium concentration,[24] which induces myogenic differentiation and cell fusion.[25-27]

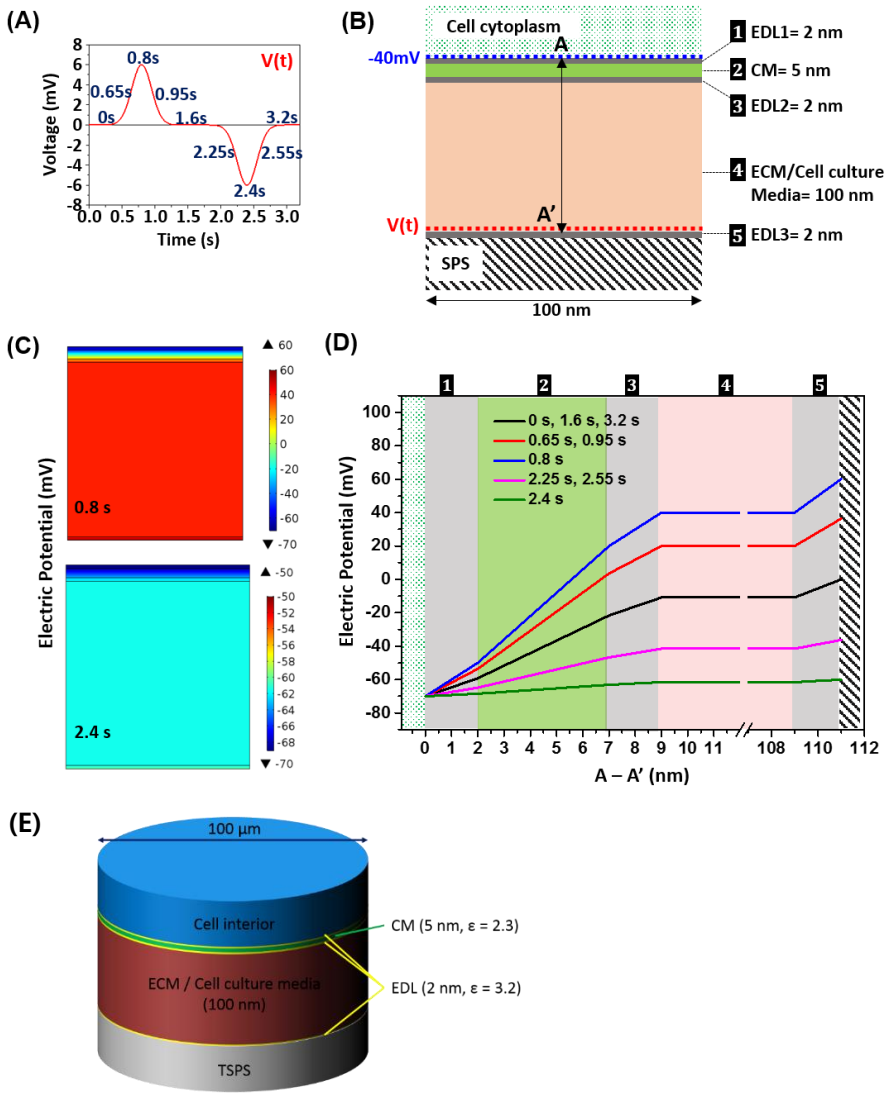

Figure 4.3. Simulation of the cell membrane potential changes due to piezoelectric potential. (A) Modeled half-electric potential as a function of time applied from the surface of TSPS. (B) The geometry of the electric potential transfer model to the cell membrane. EDL: Electrical double layer, CM: Cell membrane, ECM: extracellular matrix. (C) Calculated electric potential distributions at 0.8 and 2.4

seconds. (D) Electric potential distribution on the line A-A 'over a period. (E) Thickness and impedance of each layer, which were used to calculate the potential value transferred to cell membrane from TSPS

4.2.3. Cell sheet formation using thermosensitive pNIPAAm

To confirm pNIPAAm coating on PDMS, X-ray phoroelectron spectroscopy (XPS) was performed on PDMS, pGMA-PDMS, and pNIPAAm-pGMA-PDMS surface. First, the evidence that pGMA was coated on PDMS was the reduced silicon photoelectron peaks (Si2s, Si2p) and the increased carbon (C1s) and oxygen (O1s) photoelectron peaks on the pGMA-PDMS surface compared to the PDMS surface (Fig. 4.4A). pNIPAAm coating was confirmed by an increased nitrogen photoelectron peaks (N1s) at 401 eV with the N content of 5.26 % not seen on the surface of PDMS and pGMA-PDMS. (Fig 4.4A). The thermosensitivity of TSPS was checked by water contact angle assay in figure 4.4B, showing the hydrophilic property in low temperature (25 ℃), and hydrophobic property in higher temperature (37 ℃). Cell sheet detachment was observed after temperature change (Fig. 4.4C). The hUCBMSC-seeded and pNIPAAm-coated PDMS was cooled down to 4 ℃ by dipping in 4 ℃ PBS. The cells were detached from PDMS after 10 min, indicating that thermoresponsive pNIPAAm enabled cell sheet formation.

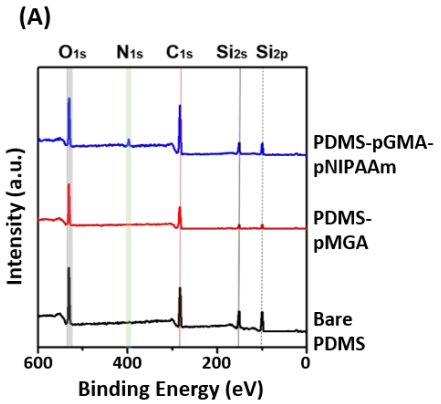

Atoms	Bare PDMS	PDMS-pMGA	PDMS-pGMA-pNIPAAm
C (%)	45.29	58.19	57.42
N (%)	0	0	5.26
O (%)	24.93	29.88	20.66
Si (%)	29.78	11.92	16.66
Total	100	100	100

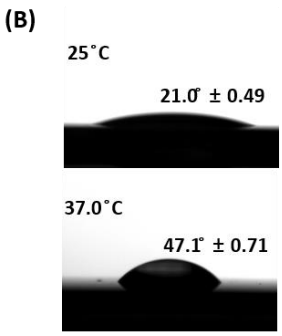

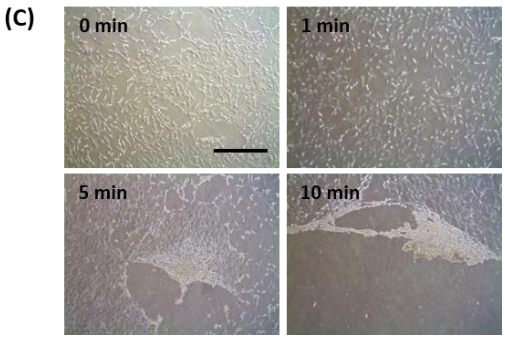

Figure 4.4. Thermosensitive properties of TSPS. (A) The chemical composition and atomic ratio of PDMS, pGMA-PDMS and pNIPAAm-pGMA-PDMS surface as analyzed by X-ray photoelectron spectroscopy. (B) Contact angle of TSPS at 25℃ and 37℃. (B) Cell detachment from TSPS by cooling down the TSPS in 4℃ PBS for 10 min

4.2.4. Enhanced myogenic differentiation of hUCBMSCs by PMEC

We investigated whether stimulating hUCBMSCs cultured on TSPS with PMEC can effectively induce myogenic differentiation. Five groups were used to evaluate the myogenic differentiation of hUCBMSCs; untreated hUCBMSCs (group A), hUCBMSCs treated with myogenic medium (group B), hUCBMSCs treated with myogenic medium and MS (group C), hUCBMSCs treated with myogenic medium and PP (group D), and hUCBMSCs treated with myogenic medium, PP and MS simultaneously (group E). Prior to evaluate the myogenic differentiation of hUCBMSCs, we first determined whether PMEC induces apoptotic effects on hUCBMSCs (Fig. 4.5A). Quantitative real time polymerase chain reaction (qPCR) of caspase-3 indicated that 3 % of MS and 120 mV of PP did not induce apoptosis of hUCBMSCs.

The gene expression of MyoD was analyzed by qPCR on day 2, 5, and 10 (Fig. 4.5B). MyoD is a transcription factor involved in early myogenesis and myoblast formation,[107] and its expression is known to decrease gradually as the myogenic differentiation further progresses.[20] Figure 4.5B showed that the gene expression of MyoD was highest on day 2 and gradually decreased until day 10 in all groups. The gene expression was highest in group E, followed by group D and C. MEF2 is also a myogenic differentiation marker and acts as an integrator of calcium ions.[108] Myogenin is related to terminal myogenic differentiation (myocyte differentiation) and cell fusion.[109] Troponin I and myosin heavy chains (Myh1 and Myh2), which are major contractile proteins in skeletal myocytes, are late-stage markers which are influenced by MRFs.[110] The expressions of these genes also were highest in group E, followed by group D and C. We confirmed the skeletal muscle-related protein expression with western blot analysis (Fig. 4.5C) and

immunocytochemistry (Fig. 4.5D). Showing similar tendency with the qPCR data, the protein expression of MyoD, myogenin, and troponin I were highest in group E, followed by group D and C.

Another important character of myogenic differentiation is cell alignment and cell fusion, which are one of terminal event during myogenesis and related with the formation of myotubes.[111] The cell alignment and cell fusion were observed by phalloidin staining which stains the F-actin of cells. Cells align perpendicularly to the direction of MS to minimize the external stress,[112-114] and this alignment was observed in group C and E (Fig. 4.5E). Cells in the other groups were not aligned, indicating that myogenic differentiation medium and PP do not induce cell alignment. Also, most cells in group E were multinucleated. Some cells in group C and D were multinucleated, in which the cells received either MS or PP. However, myogenic medium (group B) hardly induced cell fusion, indicating that MS and PP are both important factors for cell fusion, which is a character of late-stage myogenic differentiation. The late-stage myogenic differentiation was also evaluated by TEM (Fig. 4.5F). The cells only in group E had sarcomere structure. Taken together, TSPS, which provides PMEC to hUCBMSCs, can promote myogenic differentiation from early stage to late stage.

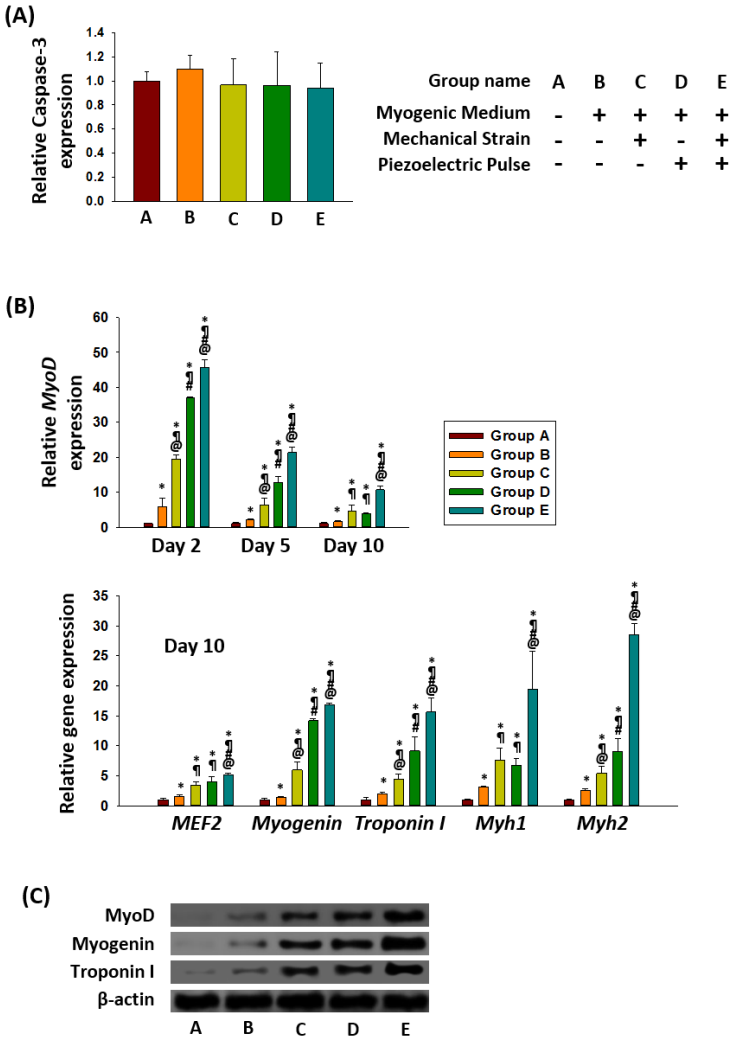
(A)
Relative Caspase-3 expression
1.4
1.2
1.0
0.8
0.6
0.4
0.2
0.0
A B C D E
Group name A B C D E
Myogenic Medium - + + + +
Mechanical Strain - - + - +
Piezoelectric Pulse - - - + +
(B)
Relative MyoD expression
60
50
40
30
20
10
0
Day 2 Day 5 Day 10
Group A
Group B
Group C
Group D
Group E
Relative gene expression
35
30
25
20
15
10
5
0
Day 10
MEF2 Myogenin Troponin I Myh1 Myh2
(C)
MyoD
Myogenin
Troponin I
β-actin
A B C D E

Figure 4.5 A-C

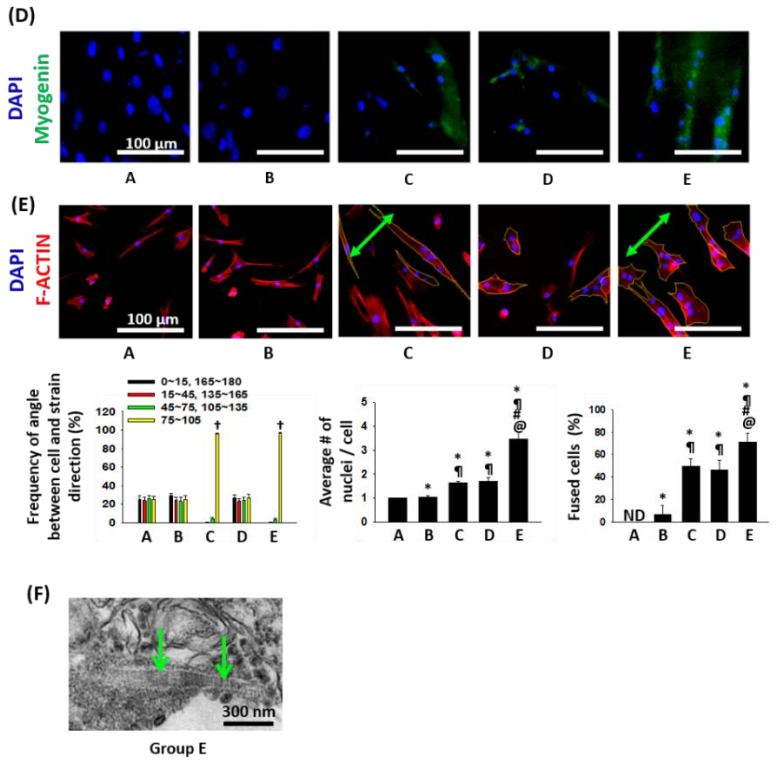

Figure 4.5. Enhanced myogenic differentiation of hUCBMSCs *in vitro* by PMEC for 10 days. (A) Gene expression of caspase-3 of hUCBMSCs *in vitro* at day 10 as evaluated by qPCR. (B) qPCR analysis for MyoD at day 2, 5 and 10, and other early-stage myogenic markers (MEF2 and Myogenin) and late-stage myogenic markers (troponin I and myosin heavy chain 1 and 2) at day 10. †$p < 0.05$ versus 45~75, 105~135, * $p < 0.05$ versus group A, ¶ $p < 0.05$ versus group B, # $p < 0.05$ versus group C, and @ $p < 0.05$ versus group D. (C) Western blot analysis for MyoD, myogenin, and troponin I. (D) Immnucytochemistry analysis for Myogenin (green). Scale bars = 100 μm. (E) Analysis of cell alignment and cell fusion by phalloidin (red) staining. Arrows indicate cyclic strain direction. †$p < 0.05$ versus 45~75, 105~135, * $p < 0.05$ versus group A, ¶ $p < 0.05$ versus group B, # $p < 0.05$ versus group C, and @ $p < 0.05$ versus group D. Scale bars = 100 μm. (F) Transmission electron microscopy of sarcomere structure in myogenic differentiated hUCBMSCs. Green arrows indicate sarcomere.

4.2.5. Intracellular signaling related to myogenic differentiation

We have investigated how PMEC induces myogenic differentiation of hUCBMSCs (Fig. 4.6A). MS induced hUCBMSC alignment (Fig. 4.5E), which is known to be critical for cell fusion to form myotubes.[115-116] MS also induces endoplasmic reticulum (ER) stress, which enhances the expression of activating transcription factor 6 (ATF6).[117] ATF6 is also known to induce cell fusion for myotube formation.[118-119] This explains a part of mechanisms by which MS induces cell fusion. MS can also enhance glucose-regulated protein 78 kDa (grp78) expression, which is known to be one of the heat shock protein (hsp) 70 family localized in ER.[120] Grp78 is known to increase MRFs expression.[121] Ras homolog family member A (RhoA), which is known to enhance the expression MRFs,[122-123] also upregulated by MS.[124]

One of the mechanisms by which PP induces cell fusion is NO_2. NO_2 is known to induce cell fusion[125-126] and be released from cells by electrical stimulation.[126] In our study, instead of NO_2 concentration in medium, the expression of neuronal nitric oxide synthase 1 (nNOS) was evaluated. Similar to upregulation of Grp78 and RhoA by MS, PP can up-regulate heat shock protein 27 (hsp27)[127] and induce phosphorylation of p38 (pp38),[128] both of which are known to enhance the expression of MRFs.[128]As shown in figure 4.6B-C, all the markers we investigated were up-regulated or induced by MS and PP.

Also, the change in V_{mem} by PMEC can be an important factor for myogenic differentiation of stem cells, as a previous study have shown that electric stimulation[129-130] and the depolarization of cells[131] can transiently up-regulate intracellular calcium concentration by opening voltage-gated calcium channel.[130] The up-regulated calcium concentration is known to promote myogenic

differentiation of C2C12 myoblasts[132-133] and myogenic cell fusion.[134] To confirm the effect of calcium influx induced by PP, we have treated a voltage-gated calcium channel blocker, nifedipine, on the cells cultured on SPS. As a result, under treatment of nifedipine, the gene expressions of MyoD and myogenin of the cells subjected to both PP and MS were remarkably decreased compared to nifedipine-negative group. Thus, we could confirm that calcium ion influx is extreamly important in skeletal myogenic differentiation using SPS.

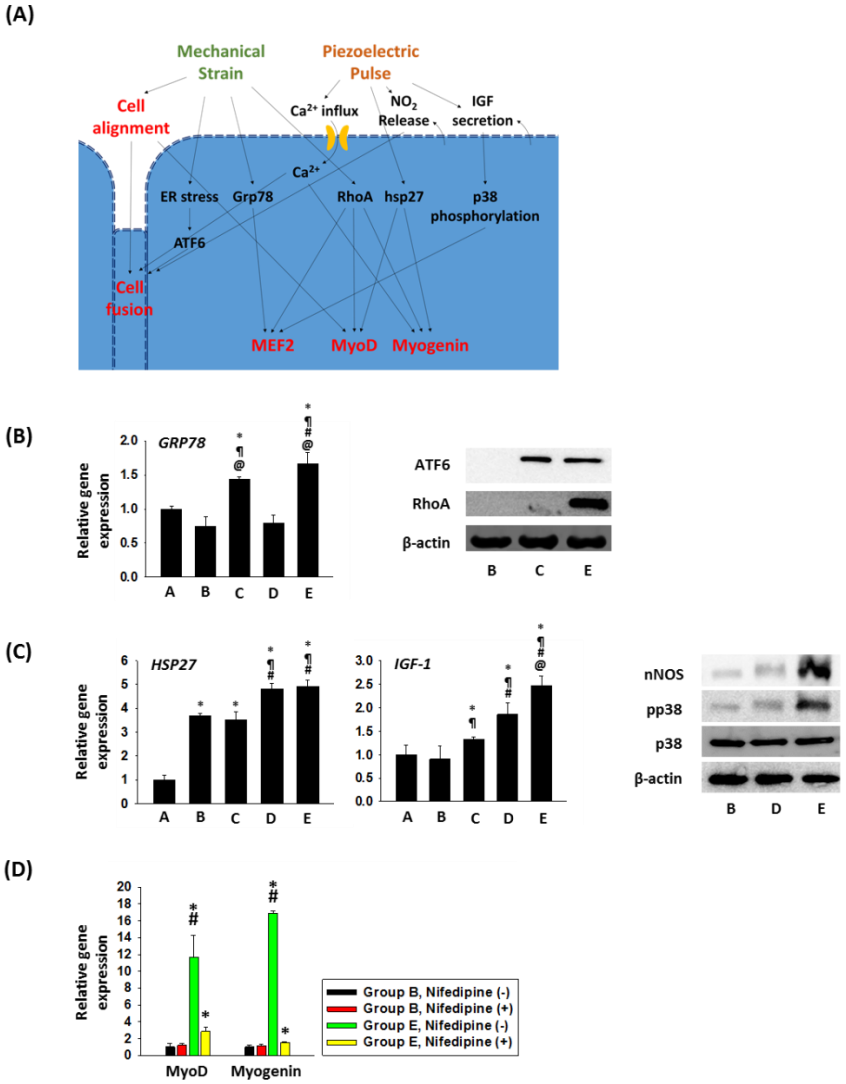

Figure 4.6. Myogenic differentiation-related intracellular signaling induced by PMEC. (A) A schematic diagram describing the myogenic differentiation-related intracellular signaling induced by MS and PP. (B) qPCR and western blot analyses for expression of myogenic differentiation-related intracellular signaling molecules induced by MS. * $p < 0.05$ versus group A, ¶ $p < 0.05$ versus group B, # $p < 0.05$ versus group C, and @ $p < 0.05$ versus group D. (C) qPCR and western blot analyses for expression of myogenic differentiation-related intracellular signaling molecules induced by PP. * p

< 0.05 versus group A, ¶ p < 0.05 versus group B, # p < 0.05 versus group C, and @ p < 0.05 versus group D. (D) qPCR of cells treated with nifedipine to block voltage-gated calcium channel. * p < 0.05 versus group B, Nifedipine (-), # p < 0.05 versus group E, Nifedipine (+).

4.2.6. Characteristics of myogenic differentiated cell sheet fragments

For intramuscular implantation of the myogenic differentiated hUCBMSC sheet fragments, first the cells were detached as cell sheets by cooling down the TSPS to 4 ℃. However, the detached cell sheets could not be injected into injured skeletal muscle with syringe because the cell sheet size was bigger than the diameter of the syringe (diameter = 200 μm). Thus, the cell sheets were spliced into smaller fragments for easy injection with syringe. The area of the cell sheet fragments and average number of nuclei per fragments were quantified (Fig. 4.7A). Also, we could confirm that the size of cell sheet fragments were not changed after the injection with syringe.

Compared to trypsinized single cells, the cell sheet fragments include a larger amounts of ECMs (Fig. 4.7B) because cells were detached from TSPS without use of protease (i.e., trypsin), which would help to prevent anoikis of the implanted cells.[30] Western blot analysis revealed that the amounts of fibronectin, laminin, collagen type I, and collagen type II were much larger in cell sheet fragments than trypsinized single cells. Major ECMs in skeletal muscle tissue are types I, III, and IV collagen, laminin, fibronectin, tenascin, and proteoglycans. These ECMs support, protect, and maintain the functional integrity of muscle fibers.[135-136] Especially, laminin and collagen type III play importants role in muscle tissue, protecting the muscle fiber from external stresses, in basal lamina and perimysium.[136-139]

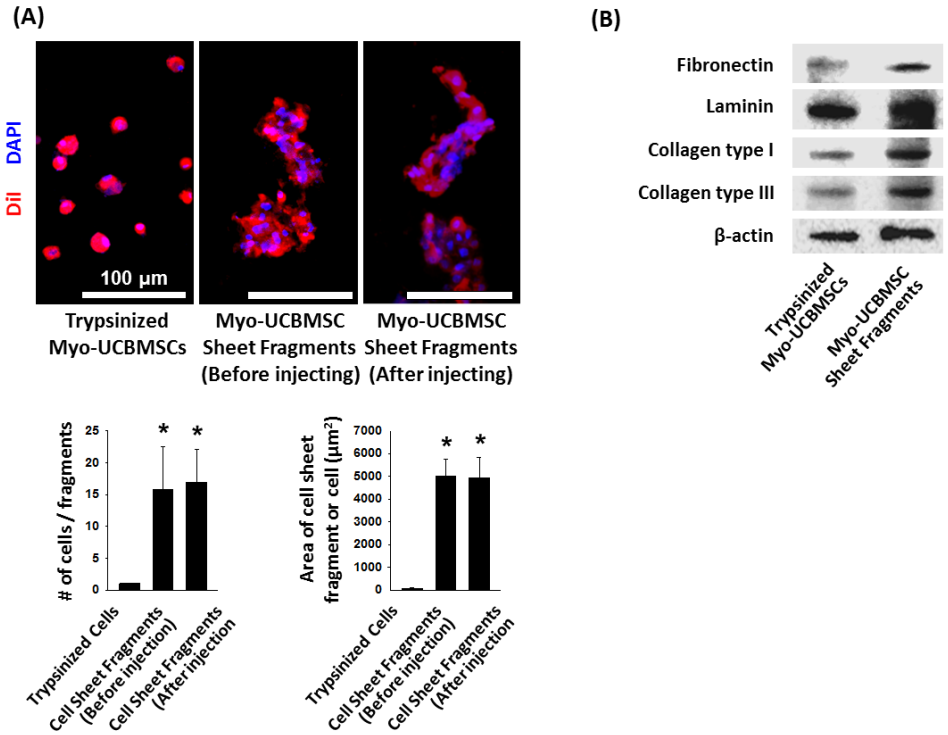

Figure 4.7. Characterization of myogenic differentiated hUCBMSCs sheet fragments. (A) DiI-labeled cells or cell sheet fragments. The fragment size and number of nuclei per fragments. Scale bars = 100 μm. * $p < 0.05$ versus the trypsinized myo-UCBMSCs group. (B) Western blot analysis for comparison of ECM contents between trypsinized cells and cell sheet fragments.

4.2.7. Improved skeletal muscle regeneration by injecting myogenic differentiated hUCBMSC sheet fragments

To evaluate skeletal muscle-regenerative effect of the myogenic differentiated hUCBMSC sheet fragments, cells were injected to the tibialis anterior (TA) muscle of CTX-induced muscle injury mice. Five groups were compared; normal TA muscle (no CTX injection, group 1) as a positive control, PBS injection (group 2) as a negative control, undifferentiated and trypsinized hUCBMSC injection (group 3), myogenic differentiated and trypsinized hUCBMSC injection (group 4), and myogenic differentiated cell sheet fragments injection (group 5). Ten days after cell transplantation, the retrieved TA muscles were stained with hematoxylin & eosin to examine the cross-sectional morphology of myofibers (Fig. 4.8A). In group 2, most of the myofibers were degenerated and a large number of inflammatory cells were observed. In group 3 and 4, a small number of myofibers with the nuclei located in the center of the myofibers were observed. Nuclei are located in the center of regenerating myofibers whereas nuclei are located in the edge of normal myofibers.[140-141] In group 5, degenerating myofibers were rarely found, and the centrally nucleated regenerating myofibers were the majority in the muscle tissue. To quantitatively evaluate muscle regeneration, we quantified the cross-sectional area of myofibers, density of regenerating myofibers with the nuclei located in the center of the myofibers, and the density of large (> 1000 μm^2) myofibers. Injection of myogenic differentiated cell sheet fragments (group 5) showed better muscle regeneration than either injection of undifferentiated and trypsinized hUCBMSCs (group 3) or injection of myogenic differentiated and trypsinized hUCBMSC (group 4).

We also performed immnohistochemistry for laminin in the CTX-induced injury TA muscle (Fig. 4.8B). Laminin is a strongly expressed ECM protein in the basement membrane of skeletal muscle and protects the myofibers from external damage.[137] In groups 2, 3 and 4, laminin expression was relatively lower and the laminin shape was not myofiber shape. In contrast, in group 5, laminin expression was higher and the laminin was well-surrounding the myofibers. To confirm the role of the transplanted cells, double staining immunohistochemistry of troponin I and human nuclear antigen (HNA) was performed (Fig. 4.8C). As a result, the expression of troponin I was higher in group 5, compared to group 3 and 4, and many cells were observed nearby, or in troponin I-positive myofiber in group 4 and 5, compared to group 3. During myogenic regeneration, a kinase named mTOR (mammalian target of rapamycin) is involved in muscle hypertrophy and prevents muscle atrophy *in vivo*.[142] We evaluated the mTOR and phosphorylated mTOR (pmTOR) protein expression (Fig. 4.8C), found that pmTOR expression was highest in group 5. Taken together, myogenic differentiated hUCBMSC sheet fragments remarkably enhanced the efficacy of MSCs for muscle regeneration. We also checked the long-term role of the injected cells by immunostaining the tissue sections of groups 4 and 5 at day 28 for desmin and HNA (Fig. 4.8E). At day 28, hUCBMSCs survived more in group 5 than in group 4. Most of the hUCBMSCs were observed in the myofibers, indicating that the implanted myogenic differentiated hUCBMSCs directly contributed to skeletal muscle regeneration.

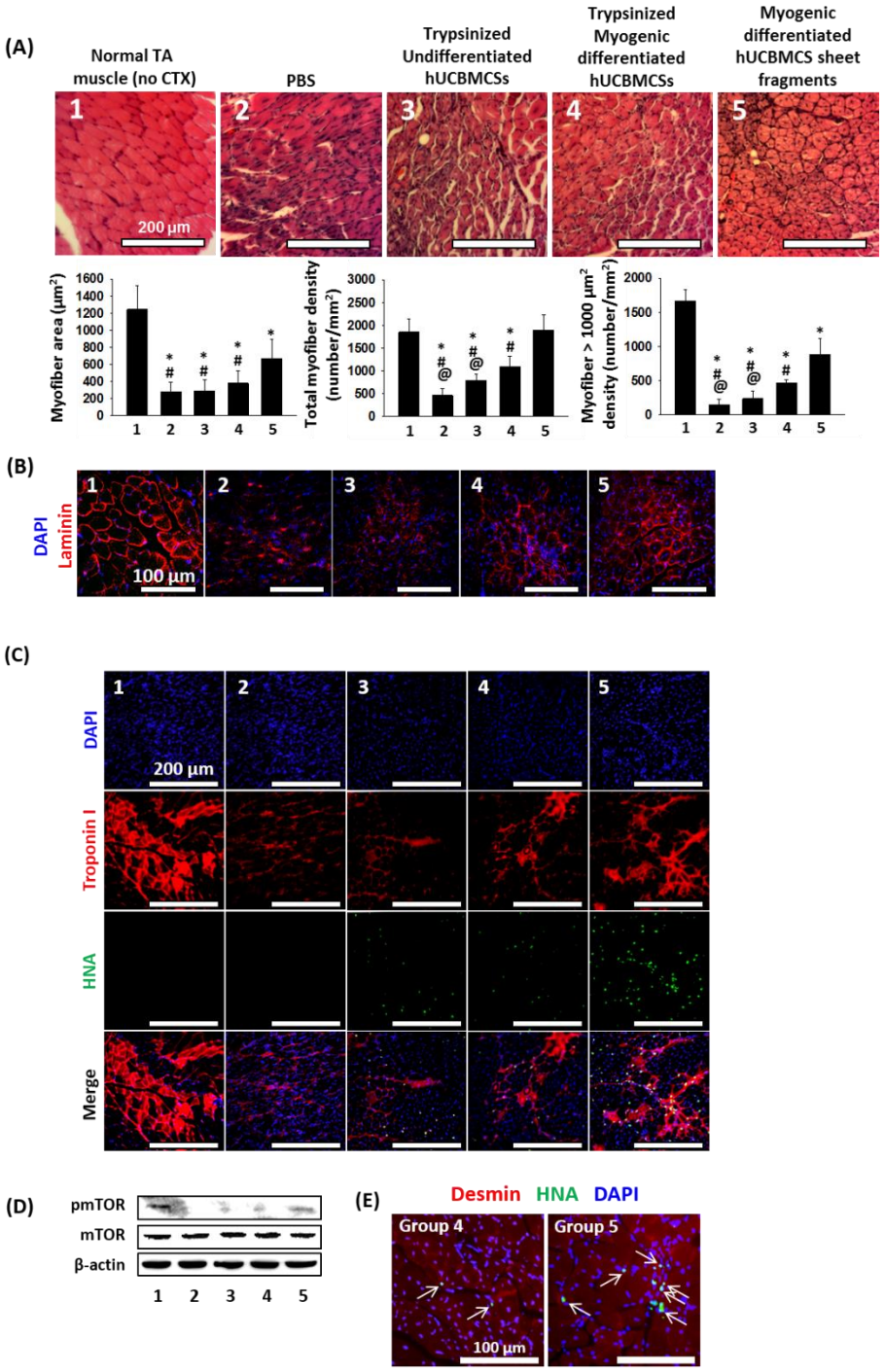
(A)
Normal TA muscle (no CTX)
PBS
Trypsinized Undifferentiated hUCBMCSs
Trypsinized Myogenic differentiated hUCBMCSs
Myogenic differentiated hUCBMCS sheet fragments
1
2
3
4
5
200 μm
Myofiber area (μm²)
Total myofiber density (number/mm²)
Myofiber > 1000 μm² density (number/mm²)
(B)
DAPI
Laminin
100 μm
(C)
DAPI
Troponin I
HNA
Merge
200 μm
(D)
pmTOR
mTOR
β-actin
1 2 3 4 5
(E)
Desmin HNA DAPI
Group 4
Group 5
100 μm

Figure 4.8. Improved skeletal muscle regeneration by injection of myogenic differentiated hUCBMSC sheet fragments 10 days after cell injection into injured muscle in mice. (A) Hematoxylin & eosin staining of TA muscle. Myofiber area, total myofiber density, and density of > 1000 μm^2 myofibers. * $p < 0.05$ versus group 1, @ $p < 0.05$ versus group 4, and # $p < 0.05$ versus group 5. (B) Immunohistochemistry for laminin (red) of TA muscle. Scale bars = 200 μm. (C) Immunohistochemistry for troponin I (red) and human nuclear antigen (HNA, green) of TA muscle. Scale bars = 200 μm. (D) Western blot analysis for mTOR and pmTOR. (E) Immnuhistochemistry staining for desmin (red) and human nuclear antigen (green) at day 28. Blue indicates DAPI. Scale bar = 100 μm. White arrows indicate the implanted cells that incorportated in myofibers.

4.2.8. Enhanced in vivo retention of hUCBMSC sheet fragments

As shown in figure 4.8, differentiated hUCBMSC sheet fragments (group 5) performed better muscle regeneration than differentiated and trypsinized hUCBMSCs (group 4). When cells are implanted *in vivo*, most of the implanted cells undergo apoptosis within a few days due to anoikis (i.e., apoptosis due to loss of cell adhesion) of the implanted cells.[30-32] Injecting cells attached to ECMs, such as three-dimensional cell spheroid[31] and cell sheets[32] is a favorable method to prevent anoikis. As the myogenic differentiated hUCBMSC sheet fragments contained more ECMs than trypsinized myogenic differentiated cells (Fig. 4.7B), the myogenic differentiated cell sheet fragments survived better for skeletal muscle regeneration following implantation.

TA muscles were immunostained for TUNEL and HNA to evaluate the retention of the injected cells in TA muscles (Fig. 4.9A). In group 3 and 4, the injected cells were randomly spread around the muscle tissue and the cell number was smaller. In contrast, in group 5, the injected cells clustered and the cell retention was approximately three times larger than that of group 3 and 4, with low apoptotic human cell ratio. The cell retention was also evaluated with *in vivo* live imaging at various time points (4, 10, 28 days after implantation) by tagging hUCBMSCs with a green fluorescent marker (Fig. 4.9B). The injected cells were more efficiently retained in group 5 compared to group 4. At day 28, most cells disappeared in group 4, while approximately half of the cells were retained in group 5. Taken together, injecting cells as cell sheet fragments would be a good method to prevent anoikis and improve cell retention following implantation.

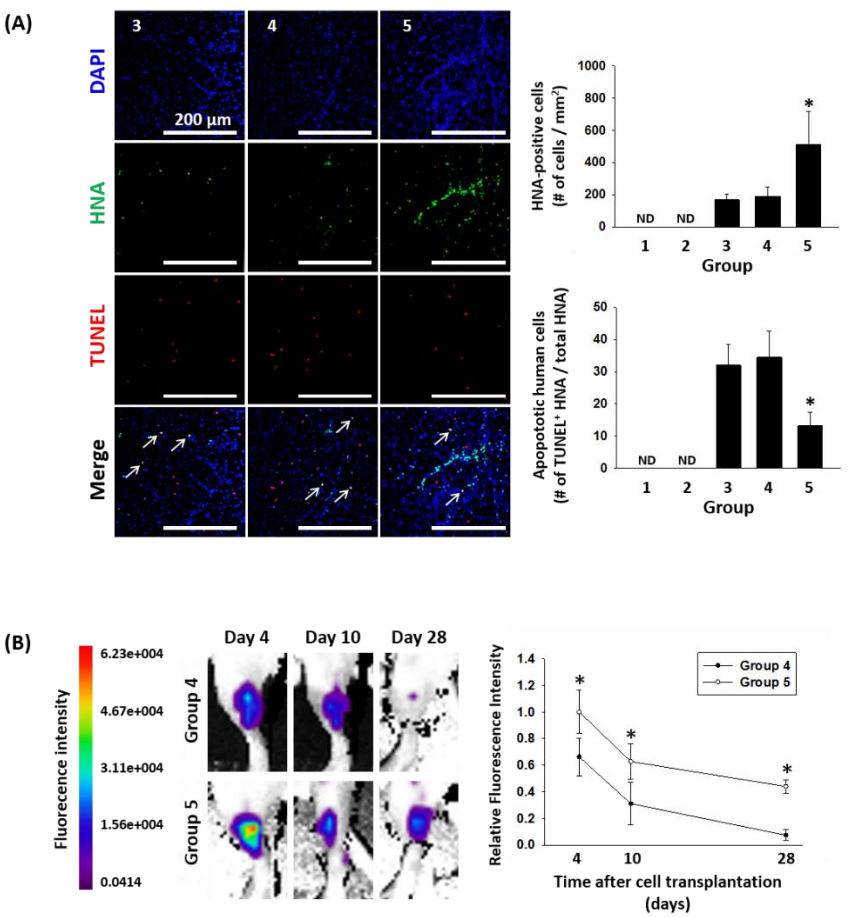

Figure 4.9. Enhanced cell retention of myogenic differentiated hUCBMSC sheet fragments injected into injured muscle in mice. (A) Immnuhistochemistry staining for human nuclear antigen (green) and TUNEL (red) at day 10. White arrows indicate TUNEL-positive HNA. Scale bars = 200 μm. The HNA-positive cell density and apoptotic human cells were quantified. * $p < 0.05$ versus group 3 and 4. (B) *In vivo* live imaging of DiO-tagged myogenic differentiated hUCBMSCs at 4, 10, and 28 days after implantation. The relative fluorescence intensity was quantified and normalized to that of group 5 at day 4. * $p < 0.05$ between group 4 and 5.

Chapter 5.

Conclusions

This studies present enhancing the cardiomyogenic and skeletal myogenic differentiation efficiency of hMSCs, for treatment of *in vivo* muscle disorders.

In chapter 3, SPS, which can mimic *in vivo* cardiac microenvironments and sequentially generate both EP and cyclic stretching signals, was developed and used as an hMSC culture substrate to maximize cardiomyogenic differentiation of hMSCs *in vitro*. EP and cyclic stretching generated by the SPS additively enhanced the *in vitro* development of cardiac phenotypes (e.g., cell alignment and expression of cardiac transcription factors, cardiac structural proteins, gap junction protein, and cardiac ion channel proteins) in hMSCs, compared to either EP, cyclic stretching, or no PMEC. EP and cyclic stretching upregulated expression of cardiomyogenic differentiation-related autocrine factors, and activated focal adhesion kinase and extracellular signal-regulated kinase signaling pathways that direct cardiomyogenic differentiation of hMSCs. SPS may be used to improve the therapeutic efficacy of hMSCs for myocardial infarction treatment, and to study electrical and mechanical regulation of stem cells.

In chapter 4, for a stem cell therapy for skeletal muscle regeneration, we developed a simple cell-culture method to generate myogenic differentiated cell-sheet fragments from hUCBMSCs. Our culture method mimicked the electrical and mechanical microenvironments of the native skeletal muscle tissue and promoted myogenic differentiation of hUCBMSCs. Following cell culture on pNIPAAm-coated substrates, cell were harvested for implantation as a cell-sheet fragment form though simple change in temperature without harmful use of trypsin. Following implantation into injured skeletal muscle in mice, myogenic differentiated hUCBMSC sheet fragments survived much better and remarkably enhanced the

efficacy of hUCBMSCs for muscle regeneration. Our culture system may be used to improve the therapeutic efficacy of stem cells for muscle diseases and to study the electrical and mechanical regulation of stem cells.

References

1. Narula, J.; Haider, N.; Arbustini, E.; Chandrashekhar, Y., Mechanisms of disease: apoptosis in heart failure--seeing hope in death. *Nat. Clin. Pract. Cardiovasc. Med.* **2006,** *3* (12), 681-8.
2. Oron, U.; Yaakobi, T.; Oron, A.; Mordechovitz, D.; Shofti, R.; Hayam, G.; Dror, U.; Gepstein, L.; Wolf, T.; Haudenschild, C.; Haim, S. B., Low-energy laser irradiation reduces formation of scar tissue after myocardial infarction in rats and dogs. *Circulation* **2001,** *103* (2), 296-301.
3. Collins, J. M.; Russell, B., Stem cell therapy for cardiac repair. *J. Cardiovasc. Nurs.* **2009,** *24* (2), 93-7.
4. Thakker, R.; Yang, P., Mesenchymal stem cell therapy for cardiac repair. *Curr. Treat. Options Cardiovasc. Med.* **2014,** *16* (7), 323.
5. Nussbaum, J.; Minami, E.; Laflamme, M. A.; Virag, J. A.; Ware, C. B.; Masino, A.; Muskheli, V.; Pabon, L.; Reinecke, H.; Murry, C. E., Transplantation of undifferentiated murine embryonic stem cells in the heart: teratoma formation and immune response. *FASEB J.* **2007,** *21* (7), 1345-57.
6. Amado, L. C.; Saliaris, A. P.; Schuleri, K. H.; St John, M.; Xie, J. S.; Cattaneo, S.; Durand, D. J.; Fitton, T.; Kuang, J. Q.; Stewart, G.; Lehrke, S.; Baumgartner, W. W.; Martin, B. J.; Heldman, A. W.; Hare, J. M., Cardiac repair with intramyocardial injection of allogeneic mesenchymal stem cells after myocardial infarction. *Proc. Natl. Acad. Sci. U. S. A.* **2005,** *102* (32), 11474-9.
7. Joggerst, S. J.; Hatzopoulos, A. K., Stem cell therapy for cardiac repair:

benefits and barriers. *Expert Rev. Mol. Med.* **2009,** *11*, e20.

8. Mauro, A., Satellite cell of skeletal muscle fibers. *J Biophys Biochem Cytol* **1961,** *9*, 493-5.

9. Wozniak, A. C.; Anderson, J. E., Nitric oxide-dependence of satellite stem cell activation and quiescence on normal skeletal muscle fibers. *Dev. Dyn.* **2007,** *236* (1), 240-50.

10. Heslop, L.; Morgan, J. E.; Partridge, T. A., Evidence for a myogenic stem cell that is exhausted in dystrophic muscle. *J. Cell Sci.* **2000,** *113 (Pt 12)*, 2299-308.

11. Law, P. K.; Goodwin, T. G.; Wang, M. G., Normal myoblast injections provide genetic treatment for murine dystrophy. *Muscle Nerve* **1988,** *11* (6), 525-33.

12. Law, P. K.; Bertorini, T. E.; Goodwin, T. G.; Chen, M.; Fang, Q. W.; Li, H. J.; Kirby, D. S.; Florendo, J. A.; Herrod, H. G.; Golden, G. S., Dystrophin production induced by myoblast transfer therapy in Duchenne muscular dystrophy. *Lancet* **1990,** *336* (8707), 114-5.

13. Mizuno, H., The potential for treatment of skeletal muscle disorders with adipose-derived stem cells. *Curr. Stem Cell Res. Ther.* **2010,** *5* (2), 133-6.

14. Makino, S.; Fukuda, K.; Miyoshi, S.; Konishi, F.; Kodama, H.; Pan, J.; Sano, M.; Takahashi, T.; Hori, S.; Abe, H., Cardiomyocytes can be generated from marrow stromal cells in vitro. *The Journal of clinical investigation* **1999,** *103* (5), 697-705.

15. Burlacu, A.; Rosca, A. M.; Maniu, H.; Titorencu, I.; Dragan, E.; Jinga, V.; Simionescu, M., Promoting effect of 5-azacytidine on the myogenic differentiation of bone marrow stromal cells. *Eur. J. Cell Biol.* **2008,** *87* (3),

173-84.

16. Li, T. S.; Hayashi, M.; Ito, H.; Furutani, A.; Murata, T.; Matsuzaki, M.; Hamano, K., Regeneration of infarcted myocardium by intramyocardial implantation of ex vivo transforming growth factor-beta-preprogrammed bone marrow stem cells. *Circulation* **2005,** *111* (19), 2438-45.

17. Bartunek, J.; Croissant, J. D.; Wijns, W.; Gofflot, S.; de Lavareille, A.; Vanderheyden, M.; Kaluzhny, Y.; Mazouz, N.; Willemsen, P.; Penicka, M.; Mathieu, M.; Homsy, C.; De Bruyne, B.; McEntee, K.; Lee, I. W.; Heyndrickx, G. R., Pretreatment of adult bone marrow mesenchymal stem cells with cardiomyogenic growth factors and repair of the chronically infarcted myocardium. *Am. J. Physiol. Heart Circ. Physiol.* **2007,** *292* (2), H1095-104.

18. Xie, X. J.; Wang, J. A.; Cao, J.; Zhang, X., Differentiation of bone marrow mesenchymal stem cells induced by myocardial medium under hypoxic conditions. *Acta Pharmacol. Sin.* **2006,** *27* (9), 1153-8.

19. Wang, T.; Xu, Z.; Jiang, W.; Ma, A., Cell-to-cell contact induces mesenchymal stem cell to differentiate into cardiomyocyte and smooth muscle cell. *Int. J. Cardiol.* **2006,** *109* (1), 74-81.

20. Gang, E. J.; Jeong, J. A.; Hong, S. H.; Hwang, S. H.; Kim, S. W.; Yang, I. H.; Ahn, C.; Han, H.; Kim, H., Skeletal myogenic differentiation of mesenchymal stem cells isolated from human umbilical cord blood. *Stem Cells* **2004,** *22* (4), 617-24.

21. Dezawa, M.; Ishikawa, H.; Itokazu, Y.; Yoshihara, T.; Hoshino, M.; Takeda, S.; Ide, C.; Nabeshima, Y., Bone marrow stromal cells generate muscle cells and repair muscle degeneration. *Science* **2005,** *309* (5732), 314-7.

22. Tian, H.; Bharadwaj, S.; Liu, Y.; Ma, H.; Ma, P. X.; Atala, A.; Zhang, Y., Myogenic differentiation of human bone marrow mesenchymal stem cells on a 3D nano fibrous scaffold for bladder tissue engineering. *Biomaterials* **2010,** *31* (5), 870-7.

23. Hou, J. F.; Zhang, H.; Yuan, X.; Li, J.; Wei, Y. J.; Hu, S. S., In vitro effects of low-level laser irradiation for bone marrow mesenchymal stem cells: proliferation, growth factors secretion and myogenic differentiation. *Lasers Surg. Med*. **2008,** *40* (10), 726-33.

24. Mooney, E.; Mackle, J. N.; Blond, D. J.; O'Cearbhaill, E.; Shaw, G.; Blau, W. J.; Barry, F. P.; Barron, V.; Murphy, J. M., The electrical stimulation of carbon nanotubes to provide a cardiomimetic cue to MSCs. *Biomaterials* **2012,** *33* (26), 6132-9.

25. Genovese, J. A.; Spadaccio, C.; Chachques, E.; Schussler, O.; Carpentier, A.; Chachques, J. C.; Patel, A. N., Cardiac pre-differentiation of human mesenchymal stem cells by electrostimulation. *Front Biosci (Landmark Ed)* **2009,** *14*, 2996-3002.

26. Shradhanjali, A.; Riehl, B. D.; Kwon, I. K.; Lim, J. Y., Cardiomyocyte stretching for regenerative medicine and hypertrophy study. *Tissue Eng. Regen. Med*. **2015,** *12* (6), 398-409.

27. Huang, Y.; Zheng, L.; Gong, X.; Jia, X.; Song, W.; Liu, M.; Fan, Y., Effect of cyclic strain on cardiomyogenic differentiation of rat bone marrow derived mesenchymal stem cells. *PLoS One* **2012,** *7* (4), e34960.

28. Asumda, F. Z., Towards the development of a reliable protocol for mesenchymal stem cell cardiomyogenesis. **2013**.

29. McCullagh, K. J.; Perlingeiro, R. C., Coaxing stem cells for skeletal muscle

repair. *Adv Drug Deliv Rev* **2015,** *84*, 198-207.

30. Lee, W.-Y.; Wei, H.-J.; Lin, W.-W.; Yeh, Y.-C.; Hwang, S.-M.; Wang, J.-J.; Tsai, M.-S.; Chang, Y.; Sung, H.-W., Enhancement of cell retention and functional benefits in myocardial infarction using human amniotic-fluid stem-cell bodies enriched with endogenous ECM. *Biomaterials* **2011,** *32* (24), 5558-5567.

31. Bhang, S. H.; Cho, S. W.; La, W. G.; Lee, T. J.; Yang, H. S.; Sun, A. Y.; Baek, S. H.; Rhie, J. W.; Kim, B. S., Angiogenesis in ischemic tissue produced by spheroid grafting of human adipose-derived stromal cells. *Biomaterials* **2011,** *32* (11), 2734-47.

32. Sekine, H.; Shimizu, T.; Dobashi, I.; Matsuura, K.; Hagiwara, N.; Takahashi, M.; Kobayashi, E.; Yamato, M.; Okano, T., Cardiac cell sheet transplantation improves damaged heart function via superior cell survival in comparison with dissociated cell injection. *Tissue Eng Part A* **2011,** *17* (23-24), 2973-80.

33. Gnecchi, M.; Danieli, P.; Cervio, E., Mesenchymal stem cell therapy for heart disease. *Vascul. Pharmacol.* **2012,** *57* (1), 48-55.

34. Jang, W. S.; Lee, T. I.; Oh, J. Y.; Hwang, S. H.; Shon, S. W.; Kim, D. H.; Xia, Y.; Myoung, J. M.; Baik, H. K., Kinetically controlled way to create highly uniform mono-dispersed ZnO sub-microrods for electronics. *J. Mater. Chem.* **2012,** *22* (38), 20719-20727.

35. Orlic, D.; Kajstura, J.; Chimenti, S.; Jakoniuk, I.; Anderson, S. M.; Li, B.; Pickel, J.; McKay, R.; Nadal-Ginard, B.; Bodine, D. M.; Leri, A.; Anversa, P., Bone marrow cells regenerate infarcted myocardium. *Nature* **2001,** *410* (6829), 701-5.

36. Stamm, C.; Westphal, B.; Kleine, H. D.; Petzsch, M.; Kittner, C.; Klinge, H.; Schumichen, C.; Nienaber, C. A.; Freund, M.; Steinhoff, G., Autologous bone-marrow stem-cell transplantation for myocardial regeneration. *Lancet* **2003,** *361* (9351), 45-6.

37. Choi, Y. H.; Kurtz, A.; Stamm, C., Mesenchymal stem cells for cardiac cell therapy. *Hum. Gene Ther.* **2011,** *22* (1), 3-17.

38. Tomita, S.; Li, R. K.; Weisel, R. D.; Mickle, D. A.; Kim, E. J.; Sakai, T.; Jia, Z. Q., Autologous transplantation of bone marrow cells improves damaged heart function. *Circulation* **1999,** *100* (19 Suppl), II247-56.

39. Mirotsou, M.; Jayawardena, T. M.; Schmeckpeper, J.; Gnecchi, M.; Dzau, V. J., Paracrine mechanisms of stem cell reparative and regenerative actions in the heart. *J. Mol. Cell. Cardiol.* **2011,** *50* (2), 280-9.

40. Makino, S.; Fukuda, K.; Miyoshi, S.; Konishi, F.; Kodama, H.; Pan, J.; Sano, M.; Takahashi, T.; Hori, S.; Abe, H.; Hata, J.; Umezawa, A.; Ogawa, S., Cardiomyocytes can be generated from marrow stromal cells in vitro. *The Journal of clinical investigation* **1999,** *103* (5), 697-705.

41. Antonitsis, P.; Ioannidou-Papagiannaki, E.; Kaidoglou, A.; Papakonstantinou, C., In vitro cardiomyogenic differentiation of adult human bone marrow mesenchymal stem cells. The role of 5-azacytidine. *Interact. Cardiovasc. Thorac. Surg.* **2007,** *6* (5), 593-7.

42. He, X. Q.; Chen, M. S.; Li, S. H.; Liu, S. M.; Zhong, Y.; McDonald Kinkaid, H. Y.; Lu, W. Y.; Weisel, R. D.; Li, R. K., Co-culture with cardiomyocytes enhanced the myogenic conversion of mesenchymal stromal cells in a dose-dependent manner. *Mol. Cell. Biochem.* **2010,** *339* (1-2), 89-98.

43. Wang, Z. L.; Song, J., Piezoelectric nanogenerators based on zinc oxide

nanowire arrays. *Science* **2006,** *312* (5771), 242-6.

44. Xu, S.; Qin, Y.; Xu, C.; Wei, Y.; Yang, R.; Wang, Z. L., Self-powered nanowire devices. *Nature nanotechnology* **2010,** *5* (5), 366-73.

45. Hu, Y.; Zhang, Y.; Xu, C.; Zhu, G.; Wang, Z. L., High-output nanogenerator by rational unipolar assembly of conical nanowires and its application for driving a small liquid crystal display. *Nano letters* **2010,** *10* (12), 5025-31.

46. Dagdeviren, C.; Yang, B. D.; Su, Y.; Tran, P. L.; Joe, P.; Anderson, E.; Xia, J.; Doraiswamy, V.; Dehdashti, B.; Feng, X.; Lu, B.; Poston, R.; Khalpey, Z.; Ghaffari, R.; Huang, Y.; Slepian, M. J.; Rogers, J. A., Conformal piezoelectric energy harvesting and storage from motions of the heart, lung, and diaphragm. *Proc Natl Acad Sci U S A* **2014,** *111* (5), 1927-32.

47. Hwang, G. T.; Park, H.; Lee, J. H.; Oh, S.; Park, K. I.; Byun, M.; Park, H.; Ahn, G.; Jeong, C. K.; No, K.; Kwon, H.; Lee, S. G.; Joung, B.; Lee, K. J., Self-powered cardiac pacemaker enabled by flexible single crystalline PMN-PT piezoelectric energy harvester. *Advanced materials* **2014,** *26* (28), 4880-7.

48. Lee, T. I.; Jang, W. S.; Lee, E.; Kim, Y. S.; Wang, Z. L.; Baik, H. K.; Myoung, J. M., Ultrathin self-powered artificial skin. *Energy Environ. Sci*. **2014,** *7* (12), 3994-3999.

49. Li, Z.; Yang, R.; Yu, M.; Bai, F.; Li, C.; Wang, Z. L., Cellular level biocompatibility and biosafety of ZnO nanowires. *J. Phys. Chem. C*. **2008,** *112* (51), 20114-20117.

50. Heo, C.; Yoo, J.; Lee, S.; Jo, A.; Jung, S.; Yoo, H.; Lee, Y. H.; Suh, M., The control of neural cell-to-cell interactions through non-contact electrical field stimulation using graphene electrodes. *Biomaterials* **2011,** *32* (1), 19-

27.

51. Du, P.; Lin, X.; Zhang, X. In *Dielectric constants of PDMS nanocomposites using conducting polymer nanowires*, Solid-State Sensors, Actuators and Microsystems Conference (TRANSDUCERS), 2011 16th International, IEEE: 2011; pp 645-648.

52. Genovese, J. A.; Spadaccio, C.; Langer, J.; Habe, J.; Jackson, J.; Patel, A. N., Electrostimulation induces cardiomyocyte predifferentiation of fibroblasts. *Biochem. Biophys. Res. Commun.* **2008,** *370* (3), 450-5.

53. Park, J. S.; Chu, J. S.; Cheng, C.; Chen, F.; Chen, D.; Li, S., Differential effects of equiaxial and uniaxial strain on mesenchymal stem cells. *Biotechnol. Bioeng.* **2004,** *88* (3), 359-68.

54. Kim, D. H.; Lipke, E. A.; Kim, P.; Cheong, R.; Thompson, S.; Delannoy, M.; Suh, K. Y.; Tung, L.; Levchenko, A., Nanoscale cues regulate the structure and function of macroscopic cardiac tissue constructs. *Proc. Natl. Acad. Sci. U. S. A.* **2010,** *107* (2), 565-70.

55. Wang, T. L.; Tseng, Y. Z.; Chang, H., Regulation of connexin 43 gene expression by cyclical mechanical stretch in neonatal rat cardiomyocytes. *Biochem. Biophys. Res. Commun.* **2000,** *267* (2), 551-7.

56. Cowan, D. B.; Lye, S. J.; Langille, B. L., Regulation of vascular connexin43 gene expression by mechanical loads. *Circ. Res.* **1998,** *82* (7), 786-93.

57. Teunissen, B. E.; Jongsma, H. J.; Bierhuizen, M. F., Regulation of myocardial connexins during hypertrophic remodelling. *Eur. Heart J.* **2004,** *25* (22), 1979-89.

58. Lurtz, M. M.; Louis, C. F., Intracellular calcium regulation of connexin43.

Am. J. Physiol. Cell Physiol. **2007,** *293* (6), C1806-13.

59. Yao, J.; Morioka, T.; Li, B.; Oite, T., Coordination of Mesangial Cell Contraction by Gap Junction–Mediated Intercellular Ca2+ Wave. *J. Am. Soc. Nephrol*. **2002,** *13* (8), 2018-2026.

60. Zhuang, J.; Yamada, K. A.; Saffitz, J. E.; Kleber, A. G., Pulsatile stretch remodels cell-to-cell communication in cultured myocytes. *Circ. Res.* **2000,** *87* (4), 316-22.

61. Ge, D.; Liu, X.; Li, L.; Wu, J.; Tu, Q.; Shi, Y.; Chen, H., Chemical and physical stimuli induce cardiomyocyte differentiation from stem cells. *Biochemical and biophysical research communications* **2009,** *381* (3), 317-21.

62. Honda, M.; Kiyokawa, J.; Tabo, M.; Inoue, T., Electrophysiological characterization of cardiomyocytes derived from human induced pluripotent stem cells. *J. Pharmacol. Sci.* **2011,** *117* (3), 149-59.

63. Aaron, R. K.; Boyan, B. D.; Ciombor, D. M.; Schwartz, Z.; Simon, B. J., Stimulation of growth factor synthesis by electric and electromagnetic fields. *Clin. Orthop. Relat. Res.* **2004,** (419), 30-7.

64. Bodamyali, T.; Bhatt, B.; Hughes, F. J.; Winrow, V. R.; Kanczler, J. M.; Simon, B.; Abbott, J.; Blake, D. R.; Stevens, C. R., Pulsed electromagnetic fields simultaneously induce osteogenesis and upregulate transcription of bone morphogenetic proteins 2 and 4 in rat osteoblasts in vitro. *Biochem. Biophys. Res. Commun*. **1998,** *250* (2), 458-61.

65. Aaron, R.; Ciombor, D.; Jones, A., Bone induction by decalcified bone matrix and mRNA of TGFb and IGF-1 are increased by ELF field stimulation. *Trans Orthop Res Soc* **1997,** *22*, 548.

66. Kim, I. S.; Song, J. K.; Zhang, Y. L.; Lee, T. H.; Cho, T. H.; Song, Y. M.; Kim, D. K.; Kim, S. J.; Hwang, S. J., Biphasic electric current stimulates proliferation and induces VEGF production in osteoblasts. *Biochim. Biophys. Acta* **2006,** *1763* (9), 907-16.

67. Standley, P. R.; Obards, T. J.; Martina, C. L., Cyclic stretch regulates autocrine IGF-I in vascular smooth muscle cells: implications in vascular hyperplasia. *Am. J. Physiol.* **1999,** *276* (4 Pt 1), E697-705.

68. Mata-Greenwood, E.; Grobe, A.; Kumar, S.; Noskina, Y.; Black, S. M., Cyclic stretch increases VEGF expression in pulmonary arterial smooth muscle cells via TGF-beta1 and reactive oxygen species: a requirement for NAD(P)H oxidase. *Am. J. Physiol. Lung Cell Mol. Physiol.* **2005,** *289* (2), L288-9.

69. Quinn, T. P.; Schlueter, M.; Soifer, S. J.; Gutierrez, J. A., Cyclic mechanical stretch induces VEGF and FGF-2 expression in pulmonary vascular smooth muscle cells. *Am. J. Physiol. Lung Cell Mol. Physiol.* **2002,** *282* (5), L897-903.

70. Neidlinger-Wilke, C.; Stalla, I.; Claes, L.; Brand, R.; Hoellen, I.; Rubenacker, S.; Arand, M.; Kinzl, L., Human osteoblasts from younger normal and osteoporotic donors show differences in proliferation and TGF beta-release in response to cyclic strain. *J. Biomech.* **1995,** *28* (12), 1411-8.

71. Webb, K.; Hitchcock, R. W.; Smeal, R. M.; Li, W.; Gray, S. D.; Tresco, P. A., Cyclic strain increases fibroblast proliferation, matrix accumulation, and elastic modulus of fibroblast-seeded polyurethane constructs. *J. Biomech.* **2006,** *39* (6), 1136-44.

72. Monzen, K.; Shiojima, I.; Hiroi, Y.; Kudoh, S.; Oka, T.; Takimoto, E.; Hayashi, D.; Hosoda, T.; Habara-Ohkubo, A.; Nakaoka, T., Bone morphogenetic proteins induce cardiomyocyte differentiation through the mitogen-activated protein kinase kinase kinase TAK1 and cardiac transcription factors Csx/Nkx-2.5 and GATA-4. *Mol. Cell. Biol.* **1999,** *19* (10), 7096-7105.

73. Monzen, K.; Hiroi, Y.; Kudoh, S.; Akazawa, H.; Oka, T.; Takimoto, E.; Hayashi, D.; Hosoda, T.; Kawabata, M.; Miyazono, K., Smads, TAK1, and their common target ATF-2 play a critical role in cardiomyocyte differentiation. *The Journal of cell biology* **2001,** *153* (4), 687-698.

74. Pimentel, R. C.; Yamada, K. A.; Kleber, A. G.; Saffitz, J. E., Autocrine regulation of myocyte Cx43 expression by VEGF. *Circ. Res.* **2002,** *90* (6), 671-7.

75. Munoz, J. P.; Collao, A.; Chiong, M.; Maldonado, C.; Adasme, T.; Carrasco, L.; Ocaranza, P.; Bravo, R.; Gonzalez, L.; Diaz-Araya, G.; Hidalgo, C.; Lavandero, S., The transcription factor MEF2C mediates cardiomyocyte hypertrophy induced by IGF-1 signaling. *Biochem. Biophys. Res. Commun.* **2009,** *388* (1), 155-60.

76. Han, J.; Yan, X.-L.; Han, Q.-H.; Li, Y.-J.; Du, Z.-J.; Hui, Y.-N., Integrin β1 subunit signaling is involved in the directed migration of human retinal pigment epithelial cells following electric field stimulation. *Ophthalmic Res.* **2010,** *45* (1), 15-22.

77. Kim, S. W.; Kim, H. W.; Huang, W.; Okada, M.; Welge, J. A.; Wang, Y.; Ashraf, M., Cardiac stem cells with electrical stimulation improve ischaemic heart function through regulation of connective tissue growth

factor and miR-378. *Cardiovasc. Res.* **2013,** *100* (2), 241-51.

78. Hammerick, K. E.; Longaker, M. T.; Prinz, F. B., In vitro effects of direct current electric fields on adipose-derived stromal cells. *Biochem. Biophys. Res. Commun.* **2010,** *397* (1), 12-7.

79. Torsoni, A. S.; Marin, T. M.; Velloso, L. A.; Franchini, K. G., RhoA/ROCK signaling is critical to FAK activation by cyclic stretch in cardiac myocytes. *American Journal of Physiology-Heart and Circulatory Physiology* **2005,** *58* (4), 1488-1496.

80. Akazawa, H.; Komuro, I., Roles of cardiac transcription factors in cardiac hypertrophy. *Circ. Res.* **2003,** *92* (10), 1079-88.

81. Le Grand, F.; Rudnicki, M. A., Skeletal muscle satellite cells and adult myogenesis. *Curr. Opin. Cell Biol.* **2007,** *19* (6), 628-33.

82. Dhawan, J.; Rando, T. A., Stem cells in postnatal myogenesis: molecular mechanisms of satellite cell quiescence, activation and replenishment. *Trends Cell Biol.* **2005,** *15* (12), 666-73.

83. Charge, S. B.; Rudnicki, M. A., Cellular and molecular regulation of muscle regeneration. *Physiol. Rev.* **2004,** *84* (1), 209-38.

84. Conboy, I. M.; Conboy, M. J.; Smythe, G. M.; Rando, T. A., Notch-mediated restoration of regenerative potential to aged muscle. *Science* **2003,** *302* (5650), 1575-7.

85. Nakamura, Y.; Miyaki, S.; Ishitobi, H.; Matsuyama, S.; Nakasa, T.; Kamei, N.; Akimoto, T.; Higashi, Y.; Ochi, M., Mesenchymal-stem-cell-derived exosomes accelerate skeletal muscle regeneration. *FEBS Lett.* **2015,** *589* (11), 1257-65.

86. Santa María, L.; Rojas, C. V.; Minguell, J. J., Signals from damaged but not

undamaged skeletal muscle induce myogenic differentiation of rat bone-marrow-derived mesenchymal stem cells. *Exp. Cell Res.* **2004,** *300* (2), 418-426.

87. Chan, J.; O'Donoghue, K.; Gavina, M.; Torrente, Y.; Kennea, N.; Mehmet, H.; Stewart, H.; Watt, D. J.; Morgan, J. E.; Fisk, N. M., Galectin-1 induces skeletal muscle differentiation in human fetal mesenchymal stem cells and increases muscle regeneration. *Stem Cells* **2006,** *24* (8), 1879-91.

88. De Bari, C.; Dell'Accio, F.; Vandenabeele, F.; Vermeesch, J. R.; Raymackers, J. M.; Luyten, F. P., Skeletal muscle repair by adult human mesenchymal stem cells from synovial membrane. *J. Cell Biol.* **2003,** *160* (6), 909-18.

89. Musina, R. A.; Bekchanova, E. S.; Belyavskii, A. V.; Grinenko, T. S.; Sukhikh, G. T., Umbilical cord blood mesenchymal stem cells. *Bull. Exp. Biol. Med.* **2007,** *143* (1), 127-31.

90. Hwang, S.-H.; Son, E.-S.; Park, Y.-J.; Lee, C.-S.; Chun, H. J., Effect of cultured medium of human umbilical cord blood-derived mesenchymal stem cells on melanogenic enzyme activity in mouse B16 melanoma cells. *Tissue Eng. Regen. Med.* **2014,** *11* (5), 414-422.

91. Zaim, M.; Karaman, S.; Cetin, G.; Isik, S., Donor age and long-term culture affect differentiation and proliferation of human bone marrow mesenchymal stem cells. *Ann. Hematol.* **2012,** *91* (8), 1175-86.

92. Ahadian, S.; Ostrovidov, S.; Hosseini, V.; Kaji, H.; Ramalingam, M.; Bae, H.; Khademhosseini, A., Electrical stimulation as a biomimicry tool for regulating muscle cell behavior. *Organogenesis* **2013,** *9* (2), 87-92.

93. Gregory, C. M.; Bickel, C. S., Recruitment patterns in human skeletal

muscle during electrical stimulation. *Phys. Ther.* **2005,** *85* (4), 358-64.

94. Lv, S.; Dudek, D. M.; Cao, Y.; Balamurali, M. M.; Gosline, J.; Li, H., Designed biomaterials to mimic the mechanical properties of muscles. *Nature* **2010,** *465* (7294), 69-73.

95. Ludin, H. P., Microelectrode study of normal human skeletal muscle. *Eur. Neurol.* **1969,** *2* (6), 340-7.

96. Sundelacruz, S.; Levin, M.; Kaplan, D. L., Role of membrane potential in the regulation of cell proliferation and differentiation. *Stem Cell Rev* **2009,** *5* (3), 231-46.

97. Konig, S.; Hinard, V.; Arnaudeau, S.; Holzer, N.; Potter, G.; Bader, C. R.; Bernheim, L., Membrane hyperpolarization triggers myogenin and myocyte enhancer factor-2 expression during human myoblast differentiation. *J. Biol. Chem.* **2004,** *279* (27), 28187-96.

98. Sundelacruz, S.; Levin, M.; Kaplan, D. L., Membrane potential controls adipogenic and osteogenic differentiation of mesenchymal stem cells. *PLoS One* **2008,** *3* (11), e3737.

99. Yúfera, A.; Olmo, A.; Daza, P.; Cañete, D., Cell biometrics based on bio-impedance measurements. In *Advanced biometric technologies*, InTech: 2011.

100. Pethig, R., Dielectric properties of body tissues. *Clin. Phys. Physiol. Meas.* **1987,** *8 Suppl A*, 5-12.

101. Kuang, W.; Nelson, S., Low-frequency dielectric properties of biological tissues: a review with some new insights. *Transactions of the ASAE-American Society of Agricultural Engineers* **1998,** *41* (1), 173-184.

102. Flemming, R. G.; Murphy, C. J.; Abrams, G. A.; Goodman, S. L.; Nealey,

P. F., Effects of synthetic micro- and nano-structured surfaces on cell behavior. *Biomaterials* **1999,** *20* (6), 573-88.

103. Ma, Z.; Kotaki, M.; Yong, T.; He, W.; Ramakrishna, S., Surface engineering of electrospun polyethylene terephthalate (PET) nanofibers towards development of a new material for blood vessel engineering. *Biomaterials* **2005,** *26* (15), 2527-36.

104. Xu, Y.; Xu, G. y.; Tang, C.; Wei, B.; Pei, X.; Gui, J. c.; Min, B. H.; Jin, C. z.; Wang, L. m., Preparation and characterization of bone marrow mesenchymal stem cell-derived extracellular matrix scaffolds. *Journal of Biomedical Materials Research Part B: Applied Biomaterials* **2015,** *103* (3), 670-678.

105. Cho, S.; Thielecke, H., Electrical characterization of human mesenchymal stem cell growth on microelectrode. *Microelectron. Eng.* **2008,** *85* (5), 1272-1274.

106. Tomaselli, V.; Shamos, M., Electrical properties of hydrated collagen. I. Dielectric properties. *Biopolymers* **1973,** *12* (2), 353-366.

107. Rudnicki, M. A.; Schnegelsberg, P. N.; Stead, R. H.; Braun, T.; Arnold, H. H.; Jaenisch, R., MyoD or Myf-5 is required for the formation of skeletal muscle. *Cell* **1993,** *75* (7), 1351-9.

108. Lu, J.; McKinsey, T. A.; Zhang, C. L.; Olson, E. N., Regulation of skeletal myogenesis by association of the MEF2 transcription factor with class II histone deacetylases. *Mol. Cell* **2000,** *6* (2), 233-44.

109. Hasty, P.; Bradley, A.; Morris, J. H.; Edmondson, D. G.; Venuti, J. M.; Olson, E. N.; Klein, W. H., Muscle deficiency and neonatal death in mice with a targeted mutation in the myogenin gene. *Nature* **1993,** *364* (6437),

501-6.

110. Allen, D. L.; Sartorius, C. A.; Sycuro, L. K.; Leinwand, L. A., Different pathways regulate expression of the skeletal myosin heavy chain genes. *J. Biol. Chem.* **2001,** *276* (47), 43524-33.

111. Horsley, V.; Pavlath, G. K., Forming a multinucleated cell: molecules that regulate myoblast fusion. *Cells Tissues Organs* **2004,** *176* (1-3), 67-78.

112. Ghazanfari, S.; Tafazzoli-Shadpour, M.; Shokrgozar, M. A., Effects of cyclic stretch on proliferation of mesenchymal stem cells and their differentiation to smooth muscle cells. *Biochem. Biophys. Res. Commun.* **2009,** *388* (3), 601-605.

113. Pennisi, C. P.; Olesen, C. G.; de Zee, M.; Rasmussen, J.; Zachar, V., Uniaxial cyclic strain drives assembly and differentiation of skeletal myocytes. *Tissue Eng Part A* **2011,** *17* (19-20), 2543-50.

114. Rabbani, M.; Janmaleki, M.; Tafazzoli-Shadpour, M.; Teymoori, M.; Rezvaninejad, S., Effects of uniaxial cyclic stretch loading on morphology of adipose derived stem cells. *Tissue Eng. Regen. Med.* **2016,** *13* (4), 396-402.

115. Wang, P. Y.; Yu, H. T.; Tsai, W. B., Modulation of alignment and differentiation of skeletal myoblasts by submicron ridges/grooves surface structure. *Biotechnol. Bioeng.* **2010,** *106* (2), 285-94.

116. Palama, I. E.; Coluccia, A. M.; Gigli, G.; Riehle, M., Modulation of alignment and differentiation of skeletal myoblasts by biomimetic materials. *Integr. Biol. (Camb.)* **2012,** *4* (10), 1299-309.

117. Jia, L. X.; Zhang, W. M.; Zhang, H. J.; Li, T. T.; Wang, Y. L.; Qin, Y. W.; Gu, H.; Du, J., Mechanical stretch-induced endoplasmic reticulum stress,

apoptosis and inflammation contribute to thoracic aortic aneurysm and dissection. *J. Pathol.* **2015,** *236* (3), 373-83.

118. Nakanishi, K.; Dohmae, N.; Morishima, N., Endoplasmic reticulum stress increases myofiber formation in vitro. *FASEB J.* **2007,** *21* (11), 2994-3003.

119. Nakanishi, K.; Sudo, T.; Morishima, N., Endoplasmic reticulum stress signaling transmitted by ATF6 mediates apoptosis during muscle development. *J. Cell Biol.* **2005,** *169* (4), 555-60.

120. Egusa, H.; Kobayashi, M.; Matsumoto, T.; Sasaki, J.; Uraguchi, S.; Yatani, H., Application of cyclic strain for accelerated skeletal myogenic differentiation of mouse bone marrow-derived mesenchymal stromal cells with cell alignment. *Tissue Eng Part A* **2013,** *19* (5-6), 770-82.

121. Olivan, S.; Martinez-Beamonte, R.; Calvo, A. C.; Surra, J. C.; Manzano, R.; Arnal, C.; Osta, R.; Osada, J., Extra virgin olive oil intake delays the development of amyotrophic lateral sclerosis associated with reduced reticulum stress and autophagy in muscle of SOD1G93A mice. *J. Nutr. Biochem.* **2014,** *25* (8), 885-92.

122. Carnac, G.; Primig, M.; Kitzmann, M.; Chafey, P.; Tuil, D.; Lamb, N.; Fernandez, A., RhoA GTPase and serum response factor control selectively the expression of MyoD without affecting Myf5 in mouse myoblasts. *Mol. Biol. Cell* **1998,** *9* (7), 1891-902.

123. Wei, L.; Zhou, W.; Croissant, J. D.; Johansen, F. E.; Prywes, R.; Balasubramanyam, A.; Schwartz, R. J., RhoA signaling via serum response factor plays an obligatory role in myogenic differentiation. *J. Biol. Chem.* **1998,** *273* (46), 30287-94.

124. Smith, P. G.; Roy, C.; Zhang, Y. N.; Chauduri, S., Mechanical stress

increases RhoA activation in airway smooth muscle cells. *Am. J. Respir. Cell Mol. Biol.* **2003,** *28* (4), 436-42.

125. Pisconti, A.; Brunelli, S.; Di Padova, M.; De Palma, C.; Deponti, D.; Baesso, S.; Sartorelli, V.; Cossu, G.; Clementi, E., Follistatin induction by nitric oxide through cyclic GMP: a tightly regulated signaling pathway that controls myoblast fusion. *J. Cell Biol.* **2006,** *172* (2), 233-244.

126. Flaibani, M.; Boldrin, L.; Cimetta, E.; Piccoli, M.; De Coppi, P.; Elvassore, N., Muscle differentiation and myotubes alignment is influenced by micropatterned surfaces and exogenous electrical stimulation. *Tissue Eng Part A* **2009,** *15* (9), 2447-57.

127. Hronik-Tupaj, M.; Rice, W. L.; Cronin-Golomb, M.; Kaplan, D. L.; Georgakoudi, I., Osteoblastic differentiation and stress response of human mesenchymal stem cells exposed to alternating current electric fields. *Biomed Eng Online* **2011,** *10*, 9.

128. Ito, H.; Kamei, K.; Iwamoto, I.; Inaguma, Y.; Kato, K., Regulation of the levels of small heat-shock proteins during differentiation of C2C12 cells. *Exp. Cell Res.* **2001,** *266* (2), 213-21.

129. Ozkucur, N.; Monsees, T. K.; Perike, S.; Do, H. Q.; Funk, R. H., Local calcium elevation and cell elongation initiate guided motility in electrically stimulated osteoblast-like cells. *PLoS One* **2009,** *4* (7), e6131.

130. Khatib, L.; Golan, D. E.; Cho, M., Physiologic electrical stimulation provokes intracellular calcium increase mediated by phospholipase C activation in human osteoblasts. *FASEB J.* **2004,** *18* (15), 1903-5.

131. Cannell, M. B.; Berlin, J. R.; Lederer, W. J., Effect of membrane potential changes on the calcium transient in single rat cardiac muscle cells. *Science*

1987, *238* (4832), 1419-23.

132. Wedhas, N.; Klamut, H. J.; Dogra, C.; Srivastava, A. K.; Mohan, S.; Kumar, A., Inhibition of mechanosensitive cation channels inhibits myogenic differentiation by suppressing the expression of myogenic regulatory factors and caspase-3 activity. *FASEB J.* **2005,** *19* (14), 1986-97.

133. Porter, G. A., Jr.; Makuck, R. F.; Rivkees, S. A., Reduction in intracellular calcium levels inhibits myoblast differentiation. *J. Biol. Chem.* **2002,** *277* (32), 28942-7.

134. Bernheim, L.; Bader, C. R., Human myoblast differentiation: Ca(2+) channels are activated by K(+) channels. *News Physiol. Sci.* **2002,** *17*, 22-6.

135. Kjaer, M., Role of extracellular matrix in adaptation of tendon and skeletal muscle to mechanical loading. *Physiol. Rev.* **2004,** *84* (2), 649-98.

136. Chiquet, M.; Matthisson, M.; Koch, M.; Tannheimer, M.; Chiquet-Ehrismann, R., Regulation of extracellular matrix synthesis by mechanical stress. *Biochem. Cell Biol.* **1996,** *74* (6), 737-44.

137. Gawlik, K. I.; Durbeej, M., Skeletal muscle laminin and MDC1A: pathogenesis and treatment strategies. *Skelet Muscle* **2011,** *1* (1), 9.

138. Myllyla, R.; Myllyla, V. V.; Tolonen, U.; Kivirikko, K. I., Changes in collagen metabolism in diseased muscle. I. Biochemical studies. *Arch. Neurol.* **1982,** *39* (12), 752-5.

139. Duance, V. C.; Restall, D. J.; Beard, H.; Bourne, F. J.; Bailey, A. J., The location of three collagen types in skeletal muscle. *FEBS Lett.* **1977,** *79* (2), 248-52.

140. Nakagawa, O.; Arnold, M.; Nakagawa, M.; Hamada, H.; Shelton, J. M.;

Kusano, H.; Harris, T. M.; Childs, G.; Campbell, K. P.; Richardson, J. A.; Nishino, I.; Olson, E. N., Centronuclear myopathy in mice lacking a novel muscle-specific protein kinase transcriptionally regulated by MEF2. *Genes Dev.* **2005,** *19* (17), 2066-77.

141. Zia, S.; Quattrocelli, M.; Di Flippo, E.; XXX, N. S.; Bosisio, F.; Sampaolesi, M.; Deprest, J.; Toelen, J., Human Amniotic Fluid Stem Cells Modulate Muscle Regeneration After Cardiotoxin Injury in Mice. *Stem Cell Res. Ther.* **2016,** *6*.

142. Bodine, S. C.; Stitt, T. N.; Gonzalez, M.; Kline, W. O.; Stover, G. L.; Bauerlein, R.; Zlotchenko, E.; Scrimgeour, A.; Lawrence, J. C.; Glass, D. J.; Yancopoulos, G. D., Akt/mTOR pathway is a crucial regulator of skeletal muscle hypertrophy and can prevent muscle atrophy in vivo. *Nat. Cell Biol.* **2001,** *3* (11), 1014-9.

요약 (국문초록)

근육 미세환경에서 전기적 자극과 기계적 자극은 활동 전위 및 근수축의 형태로 존재한다. 본 연구에서 우리는 이와 같은 근육 미세환경을 모사하여 인간유래 중간엽 줄기세포의 심근 및 골격근 분화를 촉진하는 세포 배양 시스템을 개발하였다. 중간엽 줄기세포는 생체 내 이식 후 근육 분화를 거의 하지 않기 때문에, 이식 전 중간엽 줄기세포의 근육 분화를 유도하여 근육 질환들에 대한 줄기세포 치료법의 치료 효능을 증가시키는 것이 중요하다. 근육 미세환경에서 전기적 자극과 기계적 자극은 상호 순차적인 형태로 나타나게 되는데, 아직까지 생체 외에서 이 둘을 동시에 주는 박동성 기계전기적 신호(PMEC)를 사용하여 줄기세포의 근육분화를 유도하는 연구는 존재하지 않았다. 중간엽 줄기세포에 PMEC을 가하기 위하여 압전탄성재료(SPS)가 개발되었다. SPS는 PDMS의 스핀코팅과 배열된 산화아연 나노로드의 적층구조로 이루어져 있는데, 이는 PDMS의 탄성과 산화아연 나노로드의 압전성의 시너지효과를 세포에 주기 위함이다. 본 연구에서 세포를 SPS위에 배양하고 SPS를 주기적으로 굽혀주고 당겨주게 되면 세포들이 SPS로부터 전기적, 기계적 자극을 받게 되어 근육 분화가 일어나게 되고, 관련

된 신호전달체계 인자들도 영향을 받는다는 것이 확인되었다. 인간 생체 내 근육 세포는 크게 세 종류로 분류할 수 있는데, 심근, 골격근, 그리고 평활근이다. 제 3 장에서는 인간 골수유래 중간엽 줄기세포의 심근분화를 관찰하였으며, 제 4장에서는 SPS 위에 온도감응성 물질인 pNIPAAm을 접목하여 인간 제대혈 유래 중간엽 줄기세포의 골격근 분화, 그리고 이 골격근 분화된 세포 시트 조각들을 이용한 마우스 골격근 질환 모델의 치료 효능을 관찰하였고, 분화된 세포들과 세포시트 조각이 각각 마우스 골격근 질환 모델을 치료하는데 효과가 있음을 밝혔다. 본 연구에서 개발한 새로운 세포 배양 시스템은 줄기세포에 대한 전기적, 기계적 제어에 대한 좋은 연구 기술이 될 뿐만 아니라 줄기세포 치료제의 치료 효능을 증가시키는 기술로서 가치가 있을 것이다.

주요어 : 인간 중간엽 줄기세포, 근육 분화, 근육 질환, 박동성 기계전기적 신호, 세포 시트

학번 : 2012-23270